Effect of DHODH mutation on p53 expression and osteoblast differentiation

Preliminary RHEP

Word Count: 574

Urwah Nawaz

a1654797

Declaration:

This work does not contain any material written by another person, except where due reference is given in the text, and the work has not been presented previously as a component of any other academic course.

1 Background

Miller's syndrome (MS) is a rare autosomal disorder characterised by craniofacial and postaxial limb deformities (Miller et al., 1979). The gene *DHODH* encodes dihydroorotate dehydrogenase (DHODH); mutations in this gene have been implicated in MS and results in DHODH loss-of-function (LOF) (Ng et al., 2010; Rainger et al., 2012). DHODH is a key enzyme in the *de novo* pyrimidine synthesis pathway, and links it the mitochondrial respiratory chain (MRC) (Fang et al., 2013). The mechanisms by which *DHODH* mutation results in MS phenotype are not fully understood.

DHODH inhibition causes impairment of pyrimidine synthesis, and mitochondrial dysfunction. In both cases DHODH inhibition has demonstrated a contribution to p53 stabilization (Fairus et al., 2017; Khutornenko et al., 2010; Linke et al., 1996). Analysis of *Dhodh* expression in mouse embryo showed spatio-temporal specific activity in pharyngeal arches and limb-buds, precursors to tissues affected in MS (Rainger et al., 2012) indicating DHODH mutation may specifically affect the embryo. The effect of p53 has been explored in Treacher-Collins syndrome (TCS), another craniofacial disorder. Trp53 knock-out in TCS mouse models ameliorated the craniofacial anomalies showing that p53 plays a role TCS pathology (Jones et al., 2008). Trp53 levels were linked to increased endogenous ROS production (Sakai et al., 2016). These observations indicate that p53 over-expression in embryo leads to craniofacial abnormalities. *DHODH* mutations may cause p53 up-regulation either via pyrimidine deficiency, mitochondrial dysfunction or in combination during embryonic development.

The primary phenotype associated with MS diagnosis is craniofacial and limb skeleton abnormalities. MC3T3-E1 cells have been used to show that depletion of DHODH decreased osteogenic gene expression (Fang et al., 2016). While p53 levels showed an increase in this study, its relation to osteoblast differentiation was not explored. MC3T3-E1 cells contains Osterix/SP7, a transcription factor required for proper osteoblast differentiation (Tian et al., 2012). Conditional inactivation of Osx/SP7 in cranial neural crest cells of mice has shown de-

fects in craniofacial bone development (Baek et al., 2013). Additionally, a human patient with a homozygous mutation in Osx/SP7 displayed craniofacial and limb bone deformities suggesting roles of Osx/SP7 in bone differentiation and patterning during embryonic development (Lapunzina et al., 2010). p53 is able to exert a repressive effect on Osx/SP7 leading to inhibition of osteoblast differentiation (Artigas et al., 2017). *Osx* mRNA levels show significant up-regulation between E11.5 and E13.5 during mouse embryonic development, subsequent to the increased *Dhodh* expression observed at E10.5 (Gao et al., 2004; Kaback et al., 2008; Rainger et al., 2012). Therefore one of the mechanisms by which *DHODH* mutation causes the MS phenotype is by inhibiting Osx/SP7 due to p53 over-expression during craniofacial and limb development.

2 Hypothesis, Aims and Experiment

Hypothesis: *DHODH* gene mutation causes stabilization of p53 in the embryo leading to disrupted osteoblast differentiation and bone hypoplasia by inhibiting Osterix/SP7 in Miller's syndrome.

- **Aim 1**: To check if DHODH LOF is causing p53 stabilization in the developing embryo.
- **Aim 2**: To confirm if Osx/SP7 expression during craniofacial and limb development are affected by DHODH LOF due to p53 stabilization
- **Aim 3**: To understand the pathway that causes p53 stabilization due to DHODH LOF

Mouse Model :
MS mouse model generation and other controls have been summarised in Table 1.

A skeletal analysis should be performed on E17.5 embryos to ensure that craniofacial and limb abnormalities are observed for MS model. Immunoblotting will confirm low DHODH levels in the model, described previously by Sakai et al. (2016) for TCS mouse model.

Table 1: Mice and controls for this experiment

Controls	Generated using	Group
Wildtype mouse (WT)	C57BL/6 wild type mouse	I
Dhodh(-/-) LOF mice	CRISPR-Cas9 can be used to specifically mutate the locus of mouse ortholog of DHODH to generate the same LOF alleles found Millers patients as described in Qin et al. (2016) CRISPR-Cas9 makes it easier to generate mouse models of any background.	II
Trp53+/- mice on a C57BL/6 background	Generated as previously described by Jones et al. (2008)	III
Trp53+/- mixed with Dhodh(-/-) LOF mice	The Trp53+/- mice on a C57BL/6 background will be bred with Dhodh(-/-) LOF mice as described by Jones et al. (2008) for TCS mouse model	IV
WT mouse treated with leflunomide	Leflunomide (LFN) is a known inhibitor for DHODH	V

Experiment Plan

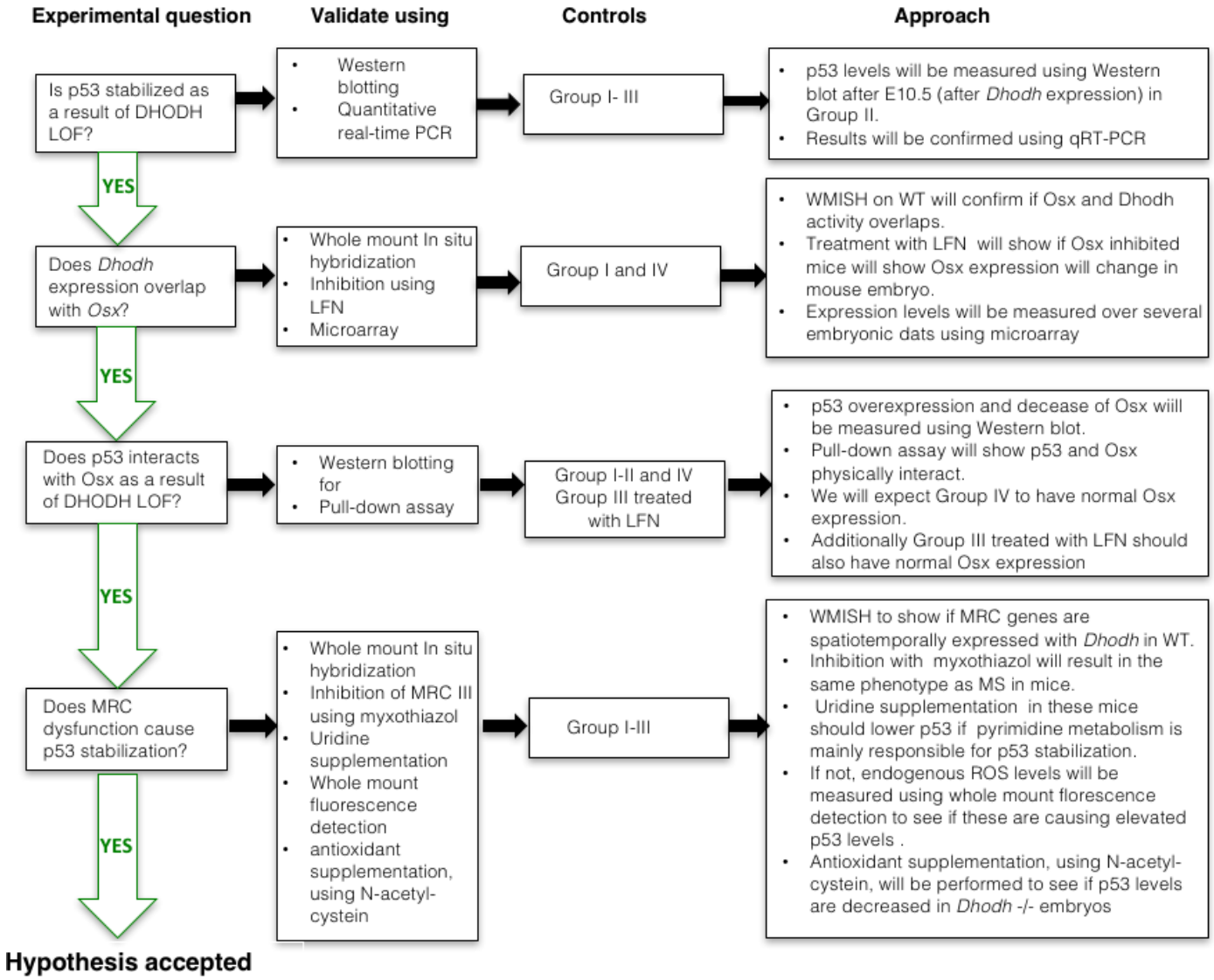

Figure 1: Experimental plan. Green arrow indicates expected results from experiments. For Control groups, refer to Table 1

References

Artigas, N., Gmez, B., Cubillos-Rojas, M., Snchez de Diego, C., Antonio Valer, J., Pons, G., Rosa, J. L., and Ventura, F. (2017). p53 inhibits SP7/Osterix activity in the transcriptional program of osteoblast differentiation.

Baek, W.-Y., Kim, Y.-J., de Crombrugghe, B., and Kim, J.-E. (2013). Osterix is required for Cranial Neural Crest-derived Craniofacial Bone Formation. *Biochemical and biophysical research communications*, 432(1):188–192.

Fairus, A. M., Choudhary, B., Hosahalli, S., Kavitha, N., and Shatrah, O. (2017). Dihydroorotate dehydrogenase (dhodh) inhibitors affect atp depletion, endogenous ros and mediate s-phase arrest in breast cancer cells. *Biochimie*, 135:154–163.

Fang, J., Uchiumi, T., Yagi, M., Matsumoto, S., Amamoto, R., Takazaki, S., Yamaza, H., Nonaka, K., and Kang, D. (2013). Dihydro-orotate dehydrogenase is physically associated with the respiratory complex and its loss leads to mitochondrial dysfunction. *Bioscience reports*, 33(2):e00021.

Fang, J., Yamaza, H., Uchiumi, T., et al. (2016). Dihydroorotate dehydrogenase depletion hampers mitochondrial function and osteogenic differentiation in osteoblasts. *European Journal of Oral Sciences*, 124(3):241–245.

Gao, Y., Jheon, A., Nourkeyhani, H., Kobayashi, H., and Ganss, B. (2004). Molecular cloning, structure, expression, and chromosomal localization of the human Osterix (SP7) gene. *Gene*, 341:101–110.

Jones, N. C., Lynn, M. L., Gaudenz, K., Sakai, D., et al. (2008). Prevention of the neurocristopathy Treacher Collins syndrome through inhibition of p53 function. *Nature Medicine*, 14(2):125–133.

Kaback, L. A., Soung, D. Y., Naik, A., Smith, N., Schwarz, E. M., O'Keefe, R. J., and

Drissi, H. (2008). Osterix/Sp7 regulates Mesenchymal stem cell mediated Endochondral Ossification. *Journal of Cellular Physiology*, 214(1):173–182.

Khutornenko, A. A., Roudko, V. V., et al. (2010). Pyrimidine biosynthesis links mitochondrial respiration to the p53 pathway. *Proceedings of the National Academy of Sciences*, 107(29):12828–12833.

Lapunzina, P., Aglan, M., Temtamy, S., Caparrós-Martín, J. A., Valencia, M., Letón, R., Martínez-Glez, V., et al. (2010). Identification of a frameshift mutation in Osterix in a patient with recessive Osteogenesis imperfecta. *The American Journal of Human Genetics*, 87(1):110–114.

Linke, S. P., Clarkin, K. C., Di Leonardo, A., Tsou, A., and Wahl, G. M. (1996). A reversible, p53-dependent g0/g1 cell cycle arrest induced by ribonucleotide depletion in the absence of detectable dna damage. *Genes & Development*, 10(8):934–947.

Miller, M., Fineman, R., and Smith, D. W. (1979). Postaxial Acrofacial Aysostosis Syndrome. *The Journal of Pediatrics*, 95(6):970–975.

Ng, S. B., Buckingham, K. J., Lee, C., et al. (2010). Exome sequencing identifies the cause of a Mendelian Disorder. *Nature Genetics*, 42(1):30–35.

Qin, W., Kutny, P. M., Maser, R. S., Dion, S. L., et al. (2016). Generating Mouse Models Using CRISPR-Cas9-Mediated Genome Editing. *Current Protocols in Mouse Biology*, pages 39–66.

Rainger, J., Bengani, H., Campbell, L., et al. (2012). Miller (genewiedemann) syndrome represents a clinically and biochemically distinct subgroup of postaxial acrofacial dysostosis associated with partial deficiency of dhodh. *Human Molecular Genetics*, 21(18):3969–3983.

Sakai, D., Dixon, J., Achilleos, A., Dixon, M., and Trainor, P. A. (2016). Prevention of Treacher Collins syndrome craniofacial anomalies in mouse models via maternal antioxidant supplementation. *Nature communications*, 7:10328.

Tian, Y., Xu, Y., Fu, Q., and Dong, Y. (2012). Osterix is required for sonic hedgehog-induced osteoblastic MC3T3-E1 cell differentiation. *Cell Biochemistry and Biophysics*, 64(3):169–176.

The Role of Dihydroorotate Dehydrogenase in Apoptosis Induction in Response to Inhibition of the Mitochondrial Respiratory Chain Complex III

A. A. Khutornenko[1], A. A. Dalina[3], B. V. Chernyak[1], P. M. Chumakov[3], A. G. Evstafieva[1, 2*]

[1]Belozersky Institute of Physico-Chemical Biology, Lomonosov Moscow State University, Leninskie Gory, 1, Bld. 40, 119991, Moscow, Russia

[2]Department of Bioengineering and Bioinformatics, Lomonosov Moscow State University, Leninskie Gory, 1, Bld. 73, 119991, Moscow, Russia

[3]Engelhardt Institute of Molecular Biology, Russian Academy of Sciences, Vavilova Str., 32, 119991, Moscow, Russia.

*E-mail: evstaf@genebee.msu.ru

Received 12.08.2013

ABSTRACT **A mechanism for the induction of programmed cell death (apoptosis) upon dysfunction of the mitochondrial respiratory chain has been studied. Previously, we had found that inhibition of mitochondrial cytochrome *bc*1, a component of the electron transport chain complex III, leads to activation of tumor suppressor p53, followed by apoptosis induction. The mitochondrial respiratory chain is coupled to the *de novo* pyrimidine biosynthesis pathway via the mitochondrial enzyme dihydroorotate dehydrogenase (DHODH). The p53 activation induced in response to the inhibition of the electron transport chain complex III has been shown to be triggered by the impairment of the *de novo* pyrimidine biosynthesis due to the suppression of DHODH. However, it remained unclear whether the suppression of the DHODH function is the main cause of the observed apoptotic cell death. Here, we show that apoptosis in human colon carcinoma cells induced by the mitochondrial respiratory chain complex III inhibition can be prevented by supplementation with uridine or orotate (products of the reaction catalyzed by DHODH) rather than with dihydroorotate (a DHODH substrate). We conclude that apoptosis is induced in response to the impairment of the *de novo* pyrimidine biosynthesis caused by the inhibition of DHODH. The conclusion is supported by the experiment showing that downregulation of DHODH by RNA interference leads to accumulation of the p53 tumor suppressor and to apoptotic cell death.**

KEYWORDS **apoptosis; p53 tumor suppressor; mitochondrial respiratory chain; dihydroorotate dehydrogenase; *de novo* pyrimidine biosynthesis.**

ABBREVIATIONS **MRC – mitochondrial respiratory chain; DHODH - dihydroorotate dehydrogenase; shRNA – short hairpin RNA; SDS – sodium dodecyl sulfate; PAAG – polyacrylamide gel; PrI – propidium iodide; FITC – fluorescein isothiocyanate.**

INTRODUCTION

Mitochondria play a central role in homeostasis in eukaryotic cells. They both supply the cell with energy by means of oxidative phosphorylation and act as important mediators of programmed cell death, as well as of the intracellular signaling cascades mediated by calcium ions and reactive oxygen species [1]. The mitochondrial respiratory chain (MRC) consists of multicomponent I-IV protein complexes integrated into the inner mitochondrial membrane, which catalyze electron transfer from NADH to molecular oxygen. This leads to the generation of the electrochemical proton gradient through the inner mitochondrial membrane, which is the driving force behind ATP synthesis by means of ATP synthase (complex V).

Many human diseases are associated with mitochondrial dysfunctions; moreover, the so-called "mitochondrial diseases" are usually caused by respiratory chain defects in these organelles [2]. Mitochondrial dysfunctions are involved in the aging process [3]. With age,

the number of mutations in mammalian mitochondrial DNA increases and respiratory chain dysfunction is observed. Cells with defects in the MRC are prone to apoptosis, and the increased cell loss is an important consequence of mitochondrial dysfunctions. In this paper we address the mechanism of apoptotic program activation upon MRC dysfunction.

The tumor suppressor p53 is a key regulatory protein that in many cases determines cell behavior in different types of stress: whether cell-cycle arrest occurs, accompanied by damage repair, or mechanisms of programmed cell death are activated, which are aimed at deleting cells with unrepairable damage [4]. Previously, we had found that the inhibition of the MRC complex III leads to an increase in the level of p53 and its activity, as well as to the activation of programmed death of human cancer cells [5]. The p53 activation appeared to be caused not by the inhibition of the MRC itself, but by the dysfunction of complex III (complex of cytochrome *bc*1) that transfers electrons from reduced ubiquinone (ubiquinol) to cytochrome *c*. One of the most important metabolic pathways in the cell, the *de novo* pyrimidine biosynthesis is coupled with the MRC [6]. The only mitochondrial enzyme of this pathway is dihydroorotate dehydrogenase (DHODH), which oxidizes dihydroorotate to orotate and uses ubiquinone as an electron acceptor [6]. The dysfunction of MRC complex III results in the transition of ubiquinone to the reduced state, which in turn may inhibit the DHODH function and lead to impairment of pyrimidine biosynthesis. Indeed, we demonstrated that an increase in the level and activity of p53 upon inhibition of the MRC complex III is due to the impairment of the DHODH function and *de novo* pyrimidine biosynthesis [5]. However, it remained unclear whether the suppression of the DHODH function is the main reason behind the activation of the cell apoptotic program upon inhibition of MRC complex III.

In this paper, we have demonstrated that impairment of the DHODH function and, as a consequence, of *de novo* pyrimidine biosynthesis induces apoptosis in human colon cancer cells upon inhibition of MRC complex III.

EXPERIMENTAL

Conditions for cell culturing and treatment

RKO and HCT116 human colon cancer cells were grown on a DMEM medium supplemented with 10% fetal bovine serum (HyClone) at 37 ^{0}C and 5% CO_2 to 50–70% confluency. Then, the cells were incubated for 12 h to determine the p53 level and for 20–26 h to analyze apoptosis in the presence of 200 nM myxothiazol (Sigma-Aldrich Inc.). In some experiments, the medium was supplemented with uridine to a final concentration of 50 μg/ml; orotate or dihydroorotate (Sigma-Aldrich Inc.) to a final concentration of 1 mM.

Evaluation of apoptosis by flow cytometry

The cells were detached from the scaffold by tryptic cleavage, washed with phosphate-buffered saline (PBS, 0.14 M NaCl; 2.7 mM KCl; 10 mM Na_2HPO_4; 1.8 mM KH_2PO_4, pH 7.3), and suspended in 100 μl of a Annexin buffer (10 mM HEPES; 140 mM NaCl; 2.5 mM $CaCl_2$, pH 7.4). Then the cells were supplemented with 7.5 μl of Annexin V conjugated to FITC (Invitrogen) and with propidium iodide (Clontech) to a final concentration of 100 μg/ml and incubated in the dark for 15 min. Thereafter, another 500 μl of the Annexin buffer was added; the cell suspension was filtered through a 30 μm filter and analyzed on a Partec PASIII flow cytometer.

Immunoblotting

The cells were lysed in a RLB buffer (Promega Inc.). Equal amounts of protein extracts (50–100 μg) were fractionated by electrophoresis in 12% SDS-PAGE; electrotransfer of the proteins onto a nitrocellulose membrane and treatment of the membrane were performed as previously described [7]. The membrane was incubated with mouse monoclonal antibodies to DHODH (ab54621, Abcam), to p53 (DO-1), or to actin (G-2) (Santa Cruz Biotechnology Inc.) diluted at a ratio of 1 : 500 with a TBST buffer (20 mM Tris-HCl, pH 7.5; 140 mM NaCl; 0.05% Tween-20) for 2 h. To control loading, the membranes were incubated with actin antibodies. Detection was performed using secondary sheep anti-mouse antibodies conjugated to horseradish peroxidase (GE Healthcare) and enhanced chemiluminescence according to the standard technique (Western Lightning Chemiluminescence Reagent, Perkin Elmer Life Sciences).

Preparation of cell lines with a reduced DHODH level

Lentiviral vectors based on the pLKO.1-puro plasmid (Sigma-Aldrich Inc.) contained the genes of short hairpin RNAs to DHODH with the following sequences: si21 – CCGGTCCGGGATTTATCAACTCAAACTCGAGTTTGA GTTGATAAATCCCGGATTTTT, si32 – CCGGCGGACTTTATAAGATGGGCTTCTCGA GAAGCCCATCTTATAAAGTCCG TTTTT.

For each lentiviral vector, pLKO-si21 and pLKO-si32, viral stocks were obtained. For this purpose, HEK293T human embryonic kidney cells on 10-cm Petri dishes were transfected with the corresponding lentiviral vector and a set of packaging plasmids [8] using LipofectAMIN 2000 (Invitrogen) according to the manufacturer's procedure. A mixture of four plasmids was used: the 3 μg lentiviral vector, 12 μg plasmid

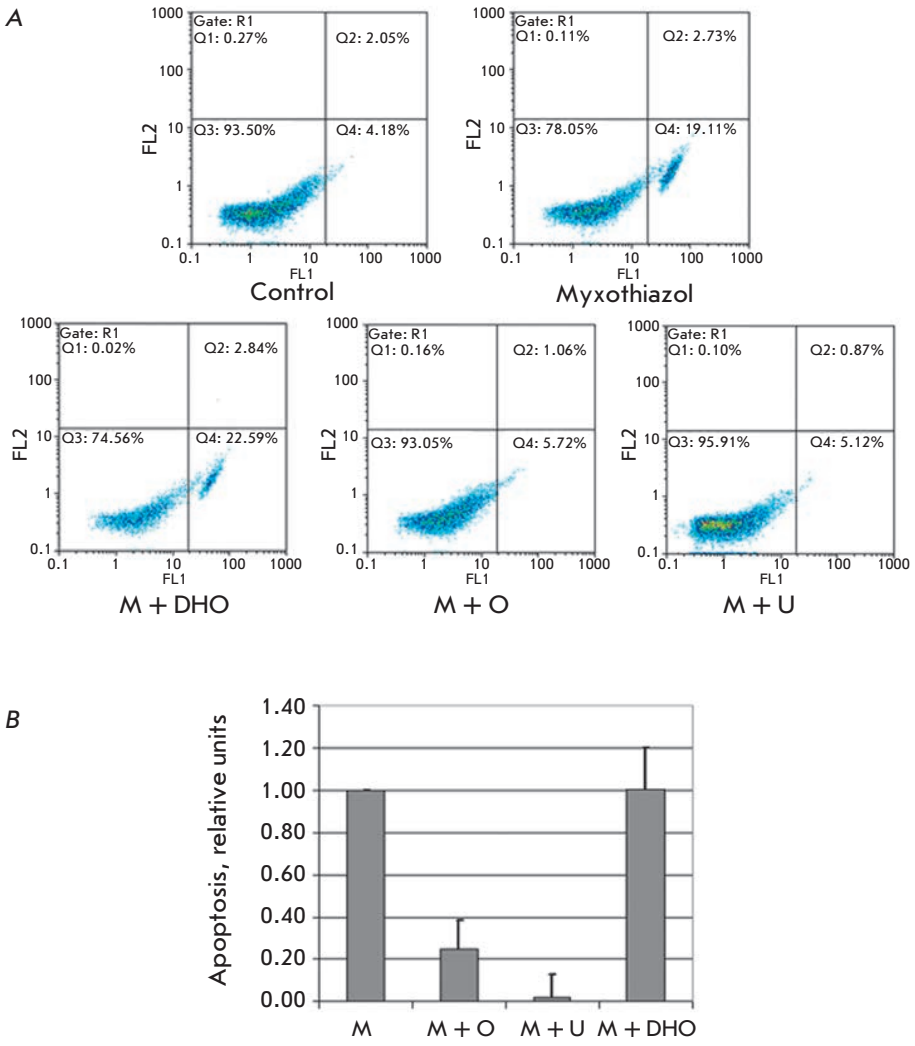

Fig. 1. Uridine and orotate, but not dihydroorotate, protect RKO cells against myxothiazol-induced apoptosis. The apoptosis level of RKO cells stained with FITC-Annexin V and PrI was determined by flow cytometry. *A* – a representative 2D diagram of cell distribution over the fluorescence intensity in FL2 (PrI) and FL1 (FITC-Annexin V) channels. Cells were analyzed 26 h after treatment with 200 nM myxothiazol (Myxothiazol, M) only or along with 1 mM dihydroorotate (M + DHO), 1 mM orotate (M + O), and 1 mM uridine (M + U). The control is untreated cells. *B* – Statistical analysis of the results. Percentage of apoptotic (AnnexinV-positive, PrI-negative) cells in each sample after subtraction of control values was normalized to the percentage of cells in which apoptosis was induced by myxothiazol without additives. The diagram shows the mean values of the relative apoptosis level and SDs of three independent experiments

pRev2 expressing the protein Rev, 6 μg plasmid pGag1 expressing the proteins Pol and Gag, and 3 μg plasmid pVSV-G expressing glycoprotein G of the vesicular stomatitis virus (a total of 24 μg DNA). The plasmid mixture, diluted with the DMEM medium, was mixed with the diluted LipofectAMIN 2000 (60 μL), stirred vigorously, incubated for 20 min at room temperature, and pipetted into a plate with the cells. On the next day, the medium was replaced with 10 ml of DMEM containing 2% fetal bovine serum.

The secreted viral particles were harvested 2 days after transfection: 10 ml of the medium from the transfected cells was filtered through a low protein binding filter (Durapore membrane, Millex-HV, Millipore) with 0.45 μm pores; 1 ml aliquots were stored at −70 °C.

RKO cells were infected with viral particles carrying two different variants of the gene of short hairpin RNA to DHODH (si32 and si21), as well as with control viruses containing no short hairpin RNA (pLS-Lpw). For this purpose, cells grown on 35-mm plates were supplemented with 1 ml of viral particles diluted in 1 ml of a fresh medium and 5–8 μg of polybrene (Hexadimethrine bromide, Sigma-Aldrich Inc.). The cells were grown in the presence of uridine (50 μg/ml). Three days later, puromycin was added (1 μg/ml) and the selection was conducted for 3 more days. The cells were lysed; the DHODH level was determined using immunoblotting.

RESULTS

The role of the impairment of pyrimidine biosynthesis in apoptosis induction upon the inhibition of the mitochondrial respiratory chain complex III

We have shown that the action of the MRC complex III inhibitors leads to growth arrest in a number of cell lines of epithelial tumors and to their massive death. A cytometric analysis of RKO human colon cancer cells

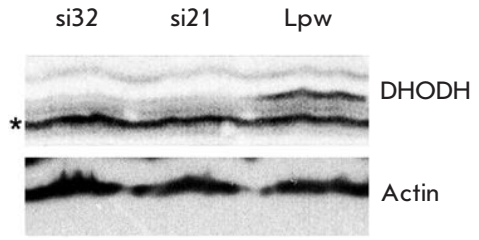

Fig. 2. Efficiency of DHODH-specific RNA interference. Western blot analysis of DHODH levels in the lysates of RKO cells infected with pLKO-si21 (si21), or with pLKO-si32 (si32), or with the empty vector pLS-Lpw (Lpw). The upper panel shows the reaction with DHODH antibodies, the lower panel shows the reaction with β-actin antibodies used as a loading control. The asterisk (*) denotes a nonspecific band, which can also serve as a sample loading control

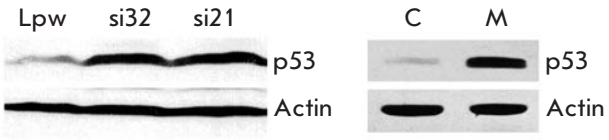

Fig. 3. DHODH interference in RKO cells results in p53 induction similarly to the effect of myxothiazol, the inhibitor of the MRC complex III. Western blot analysis of p53 levels in RKO cells infected with pLKO-si21 (si21), or with pLKO-si32 (si32), or with the empty vector pLS-Lpw (Lpw). Cells were cultured in the absence of uridine for 24 h. For comparison, the right panel shows the Western blot analysis of p53 levels in RKO cells untreated (C) or treated with 200 nM myxothiazol (M) for 12 h. Upper panel –with p53 antibodies; lower panel – with β-actin antibodies

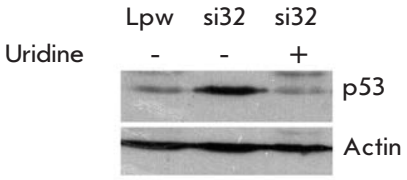

Fig. 4. Uridine prevents p53 induction in cells with DHODH knockdown. Western blot analysis of p53 levels in RKO cells infected with pLKO-si32 (si32) or with the empty vector pLS-Lpw (Lpw). Cells were cultured in the absence (–) or in the presence (+) of uridine for 24 h. Upper panel – with p53 antibodies; lower panel – with β-actin antibodies

treated with myxothiazol, an inhibitor of MRC complex III, and stained with FITC-Annexin V and propidium iodide (PrI) revealed a significant population of apoptotic cells (*Fig. 1*). In general, three cell populations were observed: normal cells (Annexin V-negative, PrI-negative), apoptotic cells (Annexin V-positive, PrI-negative, approximately 20% of all cells), and a third small population of dead cells (Annexin V-positive, PrI-positive, whose fraction was approximately 3%). The size of the third population was bigger when cells were collected not only from the scaffold, but from the medium as well (data not shown), and these cells were considered as necrotic or late-apoptotic.

Since the mitochondrial respiratory chain is functionally coupled with the *de novo* pyrimidine biosynthesis pathway via the dihydroorotate dehydrogenase inserted in the mitochondrial membrane [6], we decided to test how replenishment of the pyrimidine pool affects myxothiazol-induced apoptosis. For this purpose, a cytometric analysis was performed after treatment of RKO cells with myxothiazol in the presence of uridine. Uridine, a precursor of both uridylic and cytidylic nucleotides, appeared to almost completely prevent the accumulation of apoptotic Annexin V-positive, PrI-negative cells caused by treatment with myxothiazol (*Fig. 1*). This indicates that the reason for apoptosis induction is impairment of the *de novo* pyrimidine biosynthesis, presumably due to DHODH inhibition.

To directly assess the role of DHODH, RKO cells were treated with myxothiazol in the presence of a substrate or a product of the DHODH-catalyzed reaction; the apoptosis level was analyzed by flow cytometry. Dihydroorotate (a DHODH substrate) had no effect on myxothiazol-induced apoptosis (*Fig. 1*), but orotate (a product of the DHODH-catalyzed reaction) substantially prevented it (the number of apoptotic cells was 4 times lower than upon apoptosis induction by myxothiazol (*Fig. 1*).

Similar results were obtained for the other human colon cancer cell line, HCT116 (not shown).

The obtained data suggest that apoptosis induction upon inhibition of MRC complex III is, to a great extent, due to the DHODH inhibition and impairment of the *de novo* pyrimidine biosynthesis. For more confidence in this molecular mechanism, it was decided to conduct the reverse experiment and to check whether dysfunction of DHODH causes apoptotic cell death similarly to the inhibition of MRC complex III.

The effect of dihydroorotate dehydrogenase knockdown on tumor suppressor p53 and programmed cell death

Does dysfunction of DHODH really cause apoptotic cell death similarly to the inhibition of the MRC complex III?

To find out, it was decided to prepare a RKO cell line with DHODH expression suppressed by RNA interference. The lentiviral system was used for effective delivery of a cassette expressing short interfering RNAs. RKO cells were infected with the lentiviral particles carrying two different variants of the gene of short hairpin RNA to DHODH (si32 and si21) and also with the control viruses, which did not contain these genes (pLS-Lpw) and were grown in the presence of uridine. The cells with expression cassettes integrated into the chromosome were selected using puromycin and lysed; the DHODH level was determined using immunoblotting (*Fig. 2*).

Thus, the DHODH level in cells expressing two different short hairpin RNAs to DHODH was found to be significantly lower than in cells infected with viral particles on the basis of the "empty" vector (*Fig. 2*).

Previously, we had shown that the inhibition of MRC complex III leads to activation of the tumor suppressor p53 due to the dysfunction of DHODH [5]. To determine whether DHODH knockdown causes accumulation of p53, immunoblotting was used to compare the p53 level in the control cells and the cells with RNA interference specific to DHODH, cultured in the absence of an external uridine source. The p53 level in the cells with DHODH knockdown appeared to increase in the same way as the inhibition of the MRC complex III (*Fig. 3*).

Uridine prevented the accumulation of p53 in cells with RNA interference specific to DHODH (*Fig. 4*). Consequently, impairment of the *de novo* pyrimidine biosynthesis can be considered as the most likely cause of the increased p53 level in these cells.

Further, a cytometric analysis was performed for FITC-Annexin V and propidium iodide-stained cells with RNA interference specific to DHODH, which were cultured in the absence of an external uridine source. It turned out that an increase in the fraction of apoptotic Annexin V-positive, PrI-negative cells is the functional consequence of the suppression of DHODH expression and stabilization of p53 (*Fig. 5*). Adding uridine to the growth medium reduced the percentage of apoptotic cells to the reference level, which proves the specificity of the observed effect.

Thus, it was demonstrated by suppressing DHODH expression using the RNA interference method that both the dysfunction of DHODH and the inhibition of MRC complex III lead to elevation of the intracellular level of tumor suppressor p53 and to an increase in the level of programmed cell death (apoptosis). These results support our model, according to which apoptosis induction upon inhibition of the MRC complex III, as well as activation and stabilization of p53, occurs due to DHODH inhibition and impairment of *de novo* pyrimidine biosynthesis.

DISCUSSION

Mitochondria are the "power stations" of the cell and, simultaneously, mediators of a number of regulatory pathways, including apoptosis induction [1]. Previously, we had demonstrated that the inhibition of the MRC complex III leads to the activation of tumor suppressor p53 and to the triggering of the cell death program [5]. The activation of p53 turned out to be caused not

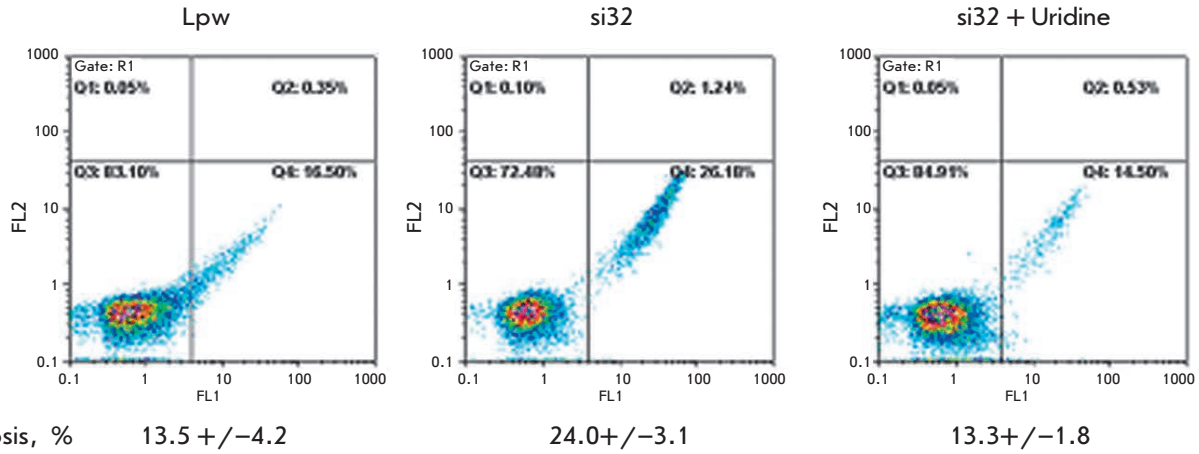

Fig. 5. Uridine protects RCO cells with DHODH knockdown against apoptosis. The apoptosis level of RKO cells, either control (Lpw) or with DHODH-specific RNA interference, cultured in the absence of an external uridine source (si32) or in the presence of uridine (si32 + uridine), was measured by flow cytometry. Cells were stained with FITC-Annexin V and propidium iodide (PrI). Results are presented as a 2D diagram of cell distribution over the fluorescence intensity in the FL2 (PrI) and FL1 (FITC-Annexin V) channels. The bottom panel shows the percentage of apoptotic (AnnexinV-positive, PrI-negative) cells (the mean value +/– SD of three independent experiments)

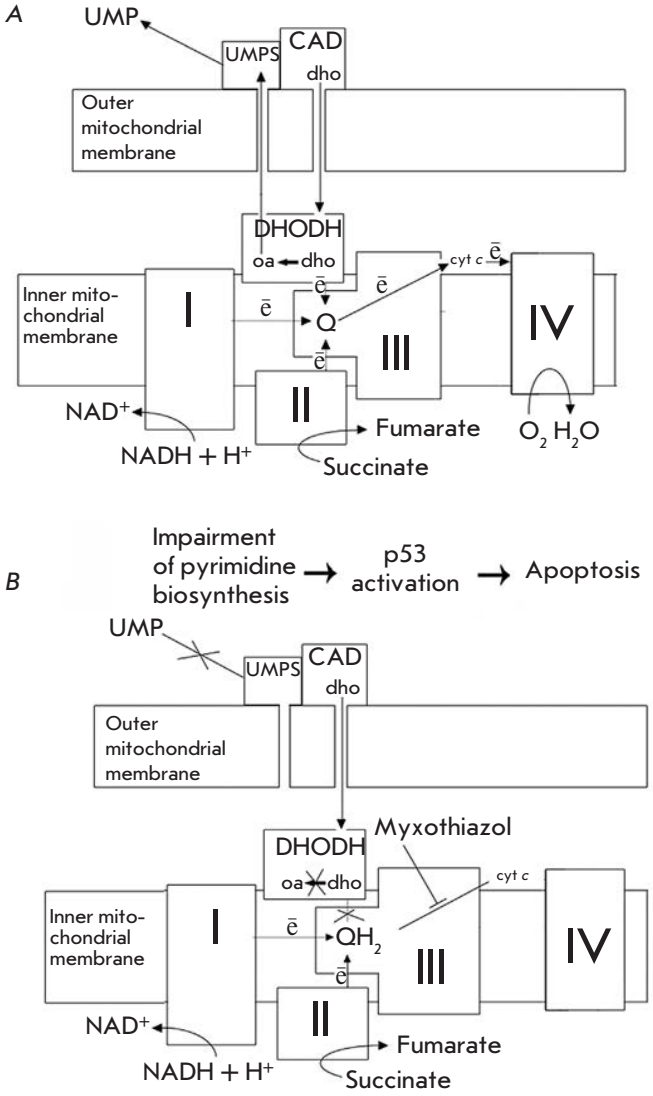

Fig. 6. A model explaining the proposed mechanism of induction of p53-dependent apoptosis in response to MRC complex III inhibition. I, II, III, IV – the MRC complexes; Q – ubiquinone; QH2 – ubiquinol; cyt *c* – cytochrome *c*; DHODH – dihydroorotate dehydrogenase; dho – dihydroorotate; oa – orotate; UMPS – uridine monophosphate synthase, UMP – uridine monophosphate, CAD – multifunction enzyme that initiates the *de novo* pyrimidine biosynthesis, OMM and IMM – outer and inner mitochondrial membranes: electrons are shown as e. *A* –untreated cells, *B* – after treatment with myxothiazol. Explanations are provided in the text

by the electron transport chain inhibition itself, but by the dysfunction of the cytochrome *bc*1 complex. It was demonstrated that this occurs due to the inhibition of dihydroorotate dehydrogenase, the only mitochondrial enzyme of the *de novo* pyrimidine biosynthesis pathway. However, it remained unknown whether the inhibition of DHODH was the exclusive cause behind the triggering of programmed cell death upon inhibition of the MRC complex III.

DHODH is a flavoprotein inserted in the inner mitochondrial membrane. DHODH oxidizes dihydroorotate to orotate and uses ubiquinone as an electron acceptor [6]. This paper demonstrates that apoptotic cell death induced by myxothiazol (an inhibitor of the MRC complex III) is fully prevented by uridine (a precursor of uridylic and cytidylic nucleotide biosynthesis) and to a large extent by orotat (a product of the reaction catalyzed by dihydroorotate dehydrogenase). Meanwhile, dihydroorotate, a DHODH substrate, does not possess this property. These data suggest that apoptotic cell death upon inhibition of the MRC complex III is in reality caused by the inhibition of DHODH, the mitochondrial enzyme of the *de novo* pyrimidine biosynthesis pathway. This conclusion is confirmed by the results of experiments on the suppression of DHODH expression using RNA interference. DHODH knockdown turned out to result in the accumulation of tumor suppressor p53 and acceleration of apoptosis.

Figure 6 provides a tentative diagram of the events resulting in apoptosis upon inhibition of the MRC complex III. Under normal conditions, ubiquinone accepts electrons from complex I, complex II, and dihydroorotate dehydrogenase. At that, ubiquinone is reduced to ubiquinol, which then donates electrons to cytochrome *c* through complex III (*Fig. 6A*). Myxothiazol-induced inhibition of MRC complex III blocks ubiquinol oxidation; ubiquinone passes to the completely reduced state and loses its ability to accept electrons during dihydroorotate oxidation. This leads to dysfunction of DHODH and, as a consequence, to impairment of *de novo* pyrimidine biosynthesis, stabilization and activation of tumor suppressor p53, and induction of programmed cell death (*Fig. 6B*). The significance of ubiquinone regeneration within the respiratory chain for *de novo* pyrimidine biosynthesis is confirmed by the fact that, as recently established, the malaria parasite *Plasmodium falciparum* apparently maintains the active mitochondrial electron transport chain exclusively for this purpose [9].

The results are in good agreement with data indicating that the DHODH inhibitor leflunomide/teriflunomide induces apoptosis in a number of human cancer cell lines [10–12]. However, according to [12], transformed keratinocytes with the mutant p53 gene, which lack transcriptionally active p53, are more sensitive to apoptosis induced by teriflunomide than normal keratinocytes with wild-type p53. In normal human epidermal keratinocytes (NHEK) a long-term exposure to teriflunomide was shown to induce cell cycle arrest at

Go/G1 due to an induction of the p53 regulated gene CDKN1A encoding the cyclin-dependent kinase inhibitor p21. The response apparently reflects a cytoprotective role for p53 against teriflunomide-induced apoptosis [12]. Treatment of human fibroblasts with PALA, another inhibitor of pyrimidine biosynthesis (N-phosphonacetyl-L-aspartate, transcarbamylase inhibitor), led to reversible cell cycle arrest, survival of cells expressing transcriptionally active p53, and apoptotic cell death in the absence of p53 [13–15]. It is assumed that under conditions of suppressed pyrimidine biosynthesis, the cytoprotective properties of p53 (promoting the survival of normal cells with wild-type p53 and death of cancer cells with inactivated p53) may be used for anti-tumor therapy employing the proper inhibitors [12].

In contrast to the published data [12–15], the present work demonstrates that the suppression of DHODH activity and impairment of *de novo* pyrimidine biosynthesis lead to apoptosis induction in human colon cancer cells expressing transcriptionally active p53. Moreover, we had previously shown that HCT116 $p53^{-/-}$ cells (cells lacking p53) demonstrate significant suppression of apoptosis compared to wild-type HCT116 cells [5]. Hence, in the studied tumor cells, p53 does not perform the cytoprotective function, but instead it promotes apoptosis induction upon impairment of *de novo* pyrimidine biosynthesis. The discrepancy between our results and the results of [12–15] may be due to tissue-specific variations and requires further study.

Our findings, as one of the consequences, suggest a possible application of inhibitors of pyrimidine biosynthesis in malignant human colon tumors expressing wild-type p53.

CONCLUSION

The mechanism of programmed cell death activation upon dysfunction of the mitochondrial respiratory chain has been investigated. It has been demonstrated that dysfunction of the mitochondrial enzyme dihydroorotate dehydrogenase, leading to blockage of the *de novo* pyrimidine biosynthesis pathway, activation of tumor suppressor p53 and, as a result, induction of p53-dependent apoptosis is the reason behind apoptosis induction in human colon cancer cells upon inhibition of the mitochondrial respiratory chain complex III.

The results disagree with the previously published data, according to which tumor suppressor p53 in human keratinocytes and fibroblasts plays the cytoprotective role and protects cells against apoptosis induced by inhibitors of pyrimidine biosynthesis. We have demonstrated that suppression of DHODH activity and impairment of *de novo* pyrimidine biosynthesis induce apoptosis in human colon cancer cells expressing transcriptionally active p53. In the studied cell lines, p53, in contrast, promoted apoptosis induction upon impairment of *de novo* pyrimidine biosynthesis. The discrepancy between our results and previously published results may be due to tissue-specific variations and requires further study. The findings suggest a possible application of inhibitors of pyrimidine biosynthesis in human colon tumors expressing wild-type p53. ●

This work was supported by the Russian Foundation for Basic Research (grants № 12-04-01444, 12-04-00538, and 12-04-32131-mol_a) and by the Federal Program "Research and Scientific-Pedagogical Personnel of Innovative Russia" (State contract P334, 2010-2012).

REFERENCES

1. McBride H.M., Neuspiel M., Wasiak S. // Curr. Biol. 2006. Vol.16. № 5. P. 551–560.
2. Meunier B., Fisher N., Ransac S., Mazat J.P., Brasseur G. // Biochim. Biophys. Acta. 2013. V. 1827. № 11–12, P. 1346–1361.
3. Trifunovic A., Larsson N.-G. // J. Intern. Med. 2008. V. 263. № 2. P.167–178.
4. Chumakov P.M. // Biochemistry (Mosc). 2007. V. 72. № 13. P.1399–1421.
5. Khutornenko A.A., Roudko V.V., Chernyak B.V., Vartapetian A.B., Chumakov P.M., Evstafieva A.G. // Proc. Natl. Acad. Sci. U S A. 2010. V.107. № 29. P. 12828–12833.
6. Evans D.R., Guy H.I. // J. Biol. Chem. 2004. V. 279. № 32. P. 33035–33038.
7. Sukhacheva E.A., Evstafieva A.G., Fateeva T.V., Shakulov V.R., Efimova N.A., Karapetian R.N., Rubtsov Y.P., Vartapetian A.B. // J. Immunol. Methods. 2002. V. 266. №1–2. P. 185–196.
8. Guryanova O.A., Makhanov M., Chenchik A.A., Chumakov P.M., Frolova E.I. // Mol. Biol. (Mosk). 2006. V. 40. № 3. P. 396–405.
9. Painter H.J., Morrisey J.M., Mather M.W., Vaidya A.B. // Nature. 2007. V. 446. № 1. P. 88–91.
10. Baumann P., Mandl-Weber S., Völkl A., Adam C., Bumeder I., Oduncu F., Schmidmaier R. // Mol. Cancer Ther. 2009. V. 8. № 3. P. 366–375.
11. Hail N.Jr., Chen P., Bushman L.R. // Neoplasia. 2010. V. 12. № 4. P. 464–475.
12. Hail N.Jr, Chen P., Kepa J.J., Bushman L.R. // Apoptosis. 2012. V. 17. № 2. P. 258–268.
13. Agarwal M.L., Agarwal A., Taylor W.R., Chernova O., Sharma Y., Stark G.R. // Proc. Natl. Acad. Sci. U S A. 1998. V. 95. № 25. P. 14775–14780.
14. Agarwal M.K., Hastak K., Jackson M.W., Breit S.N., Stark G.R., Agarwal M.L. // Proc. Natl. Acad. Sci. U S A. 2006. V. 103. № 44. P. 16278–16283.
15. Hastak K., Paul R.K., Agarwal M.K., Thakur V.S., Amin A.R., Agrawal S., Sramkoski R.M., Jacobberger J.W., Jackson M.W., Stark G.R., Agarwal M.L. // Proc. Natl. Acad. Sci. USA. 2008. V. 105. № 17. P. 6314–6319.

Cell Death and Differentiation (2017) 24, 2022–2031
 1350-9047/17

www.nature.com/cdd

p53 inhibits SP7/Osterix activity in the transcriptional program of osteoblast differentiation

Natalia Artigas[1], Beatriz Gámez[1], Mónica Cubillos-Rojas[1], Cristina Sánchez-de Diego[1], José Antonio Valer[1], Gabriel Pons[1], José Luis Rosa[1] and Francesc Ventura*[,1]

Osteoblast differentiation is achieved by activating a transcriptional network in which *Dlx5*, *Runx2* and *Osx/SP7* have fundamental roles. The tumour suppressor p53 exerts a repressive effect on bone development and remodelling through an unknown mechanism that inhibits the osteoblast differentiation programme. Here we report a physical and functional interaction between *Osx* and *p53* gene products. Physical interaction was found between overexpressed proteins and involved a region adjacent to the OSX zinc fingers and the DNA-binding domain of p53. This interaction results in a p53-mediated repression of OSX transcriptional activity leading to a downregulation of the osteogenic programme. Moreover, we show that p53 is also able to repress key osteoblastic genes in *Runx2*-deficient osteoblasts. The ability of p53 to suppress osteogenesis is independent of its DNA recognition ability but requires a native conformation of p53, as a conformational missense mutant failed to inhibit OSX. Our data further demonstrates that p53 inhibits OSX binding to their responsive Sp1/GC-rich sites in the promoters of their osteogenic target genes, such as *IBSP* or *COL1A1*. Moreover, p53 interaction to OSX sequesters OSX from binding to DLX5. This competition blocks the ability of OSX to act as a cofactor of DLX5 to activate homeodomain-containing promoters. Altogether, our data support a model wherein p53 represses OSX–DNA binding and DLX5–OSX interaction, and thereby deregulates the osteogenic transcriptional network. This mechanism might have relevant roles in bone pathologies associated to osteosarcomas and ageing.
Cell Death and Differentiation (2017) **24,** 2022–2031; doi:10.1038/cdd.2017.113; published online 4 August 2017

Osteoblast differentiation is triggered by a variety of intra- and extracellular osteogenic signals, such as BMPs, IGFs and Wnts.[1] The process commences with a mesenchymal stem cell (MSC) precursor becoming an osteochondroprogenitor cell, which is later sequentially transformed into a mature osteoblast.

It is also well known that osteochondroprogenitor maturation and the subsequent conversion of pre-osteoblasts to mature osteoblasts is controlled by a network of specific transcription factors. Among these, *Runx2* and *Osterix/SP7* (*Osx)* have a critical role in osteogenesis.[2,3] *Runx2* deletion in mice causes a severe impairment in the development of the skeleton and *Runx2* mutations in humans are causative of cleidocranial dysplasia disorder.[4] Similarly, *Osx* deletion impairs the consecution of a mature osteoblast phenotype and was proven to be important in the maintenance of bone homeostasis, because its postnatal deletion causes loss of bone mass and bone defects.[5,6] Several studies also found that *SP7/Osx* mutations or SNPs are related to osteoporosis and *osteogenesis imperfecta*.[7,8] For these reasons, *Osx* and *Runx2* are mandatory for the development of the skeleton. Moreover, both cooperatively regulate the expression of key genes in bone biology forming a transcriptional complex.[9] OSX also acts as a necessary cofactor for DLX family of transcription factors.[10] Furthermore, these transcription factors are subjected to fine tuning by posttranscriptional regulation. For instance, MAP kinases phosphorylate DLX5, RUNX2 and OSX, leading to their activation.[11–13] These studies highlighted the complexity of the transcription factor network, which controls the osteoblast differentiation process and bone development.

Maturation of MSCs to the osteoblastic phenotype is a multistep process that requires cell expansion, differentiation and survival. The tumour suppressor p53 is considered a master regulator of proliferation and apoptosis. p53 activity helps to eliminate damaged cells, preventing tumorigenesis.[14] Furthermore, p53 has been linked to cell differentiation in a variety of cell types, such as neurons, muscular cells and osteoblasts.[15–17] Surprisingly, despite the key cellular functions of p53, *Trp53* knockout mice did not show major developmental defects. However, detailed studies demonstrated skeletal abnormalities in some animals, such as upper incisor fusion and craniofacial and limb malformations.[18] *Trp53* knockout mice are also characterized by a denser skeleton than their wild-type littermates and the *Trp53*-deficient bone marrow-derived MSCs (BM-MSCs) have a higher capacity to differentiate towards the osteoblastic fate.[17,19] The impact of p53 on the osteoblastic transcription factor network is also evident, as cells with the *Trp53* deletion overexpress *Osx* and osteogenic genes through an unknown mechanism.[17]

Previous studies suggested that *p53* deletion allows overactivation of the BMP pathway by mechanisms that involve changes in the expression of *Smad1* or *Smurf1*.[20,21] It has also been shown that p53 and RUNX2 proteins interact, blocking Runx2 transcriptional activity, and that p53 regulates *Runx2*

[1]Departament de Ciències Fisiològiques, Universitat de Barcelona, IDIBELL, L'Hospitalet de Llobregat, Spain

*Corresponding author: Francesc Ventura, Departament de Ciències Fisiològiques, Universitat de Barcelona, IDIBELL, C/Feixa Llarga s/n, E-08907 L'Hospitalet de Llobregat, Spain. Tel: +34 934024281; Fax: +34 934024268; E-mail: fventura@ub.edu

Received 23.9.16; revised 21.4.17; accepted 12.6.17; Edited by S Fulda; published online 04.8.17

expression levels by an miRNA-mediated mechanism.[22,23] Therefore, although the inhibitory role of p53 in bone formation is well established, little is yet known about the molecular mechanisms by which p53 exerts this function. Moreover, an in-depth understanding of the role of p53 in bone biology could have implications in the knowledge of pathologies associated with p53 signalling network alterations.

Our work focused in the identification of the molecular mechanisms by which p53 exerts a repressive effect over the osteoblast differentiation programme. We found, using either loss- or gain-of-function models, that p53 expression has a negative impact on the expression of osteoblast-specific transcription factors and their targets. Our work further demonstrated that the negative role of p53 is independent of p53 transcriptional activity but instead required physical interaction between OSX and p53 at the protein level. p53 prevented OSX from binding to Sp1/GC-rich sequences and blocked OSX from interacting with DLX5 and binding to homeodomain sequences.

Results

p53 downregulates osteoblastic gene expression. It has been previously established that p53 has an inhibitory role in osteoblast differentiation using mouse models.[17,24] There is also evidences suggesting that these phenotypes are cell autonomous, as the BM-MSCs from *p53*-deficient mice show enhanced differentiation *in vitro*.[19] To further characterize the molecular mechanism underlying these phenotypes, we first evaluated osteoblastic gene expression from primary osteoblasts obtained from *Trp53* knockout or wild-type mice. Absence of p53 results in upregulation of important genes implicated in bone development (Figure 1a). Importantly, two transcription factors with relevant roles in bone biology, *Dlx5* and *Osx*,[11,25] were 2-fold and 3.5-fold overexpressed, respectively. Furthermore, *Runx2* showed a slight upregulation at the mRNA level. OSX target genes were also upregulated in *Trp53* knockout osteoblasts, such as *Ibsp* (bone sialoprotein) or *Bglap* (osteocalcin).[9,26,27]

To confirm these results, we used the p53-inducible SaOs2 cell line SaOs2-p53TetOn, which only expresses p53 upon the addition of doxycycline (Figure 1b). Treatment with doxycycline for 24 h confirmed the p53-dependent inhibition of O*SX*, *DLX5*, *IBSP* and *COL1A1* expression. The upregulation of *BGLAP* expression after induction of p53 expression could be explained by direct binding of p53 to the known p53-responsive sequences in *BGLAP* promoter.[28,29] These results provide evidence of a p53-dependent downregulation of the expression of osteoblastic genes.

As previous studies had identified the involvement of the osteogenic BMP pathway on p53's effects, we next focused on this signalling pathway and its modulation by p53. As previously reported, p53 deletion results in a slight upregulation of *Smad1* mRNA, as well as the BMP-target gene *Id1* in primary osteoblasts [16,30] (Supplementary Figure 1A, left panel). Interestingly, an induction of *Smad7* was found in p53 knockout osteoblast. In accordance a 1.4-fold upregulation of *SMAD7* expression was obtained after induction of p53

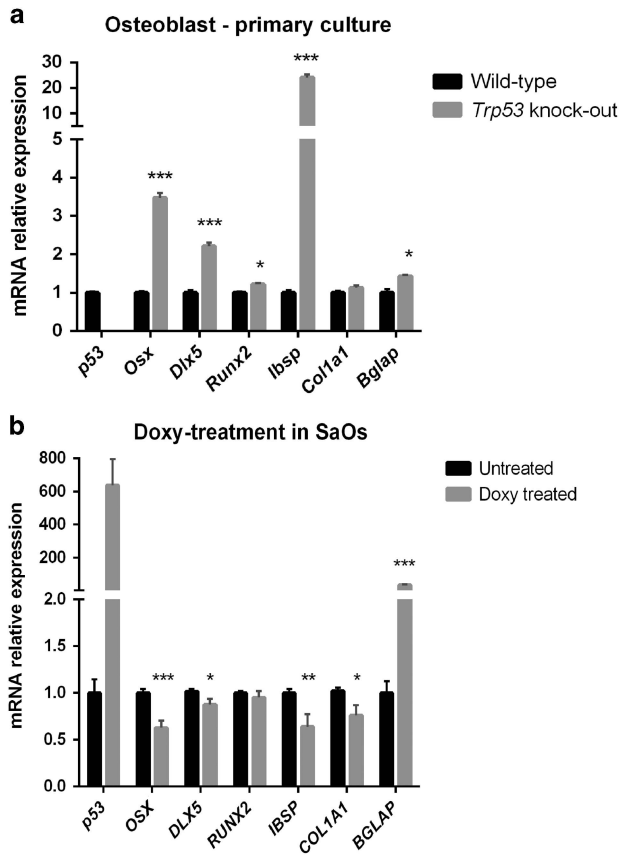

Figure 1 p53 protein inhibits osteogenic differentiation transcriptional programme. (**a**) mRNA expression levels of primary osteoblasts from wild-type or *Trp53* knockout mice grown for 3 days in osteogenic differentiation medium, and (**b**) SaOs2-p53TetOn were treated for 24 h with doxycycline 2 nM in 1% FBS medium. *Bglap* indicates *Osteocalcin* gene mRNA. mRNAs were measured by RT-qPCR, normalized to *TBP* and expressed as relative expression ± S.E.M. of at least three independent experiments (*$P<0.05$, **$P<0.01$, ***$P<0.001$, using the Student's *t*-test)

in SaOs2 cells, but no substantial changes in the expression of *SMAD1* or *ID1* (Supplementary Figure 1A, right panel).

SaOs2-p53TetOn cells were also incubated with doxycycline for 16 h and treated with 2 nM BMP2 for 2 h. Our results failed to detect significant differences in pSMAD1/5/8 levels in either primary osteoblasts or the SaOs2-p53TetOn model (Supplementary Figures 1B and C). Moreover, expression of genes such as *JUNB*, *SMAD7* or *DLX5*, which are direct targets of Smad-transcription factors, was independent of p53 induction and only *ID1* displayed a minor downregulation in the doxycycline-treated condition (Supplementary Figure 1D). Thus, these minor negative effects of p53 on the BMP pathway likely could not explain the changes observed in osteogenic gene expression.

p53 physically interacts with Osx. In order to identify the mechanisms involved in inhibition of osteogenic gene expression by p53 we focused on two drivers of bone development, RUNX2 and OSX. As a mechanism by which p53 inhibits RUNX2 through physical interaction has been described previously in a DNA-damage context,[22] we also tested the capacity of p53 to bind to RUNX2 and OSX. To

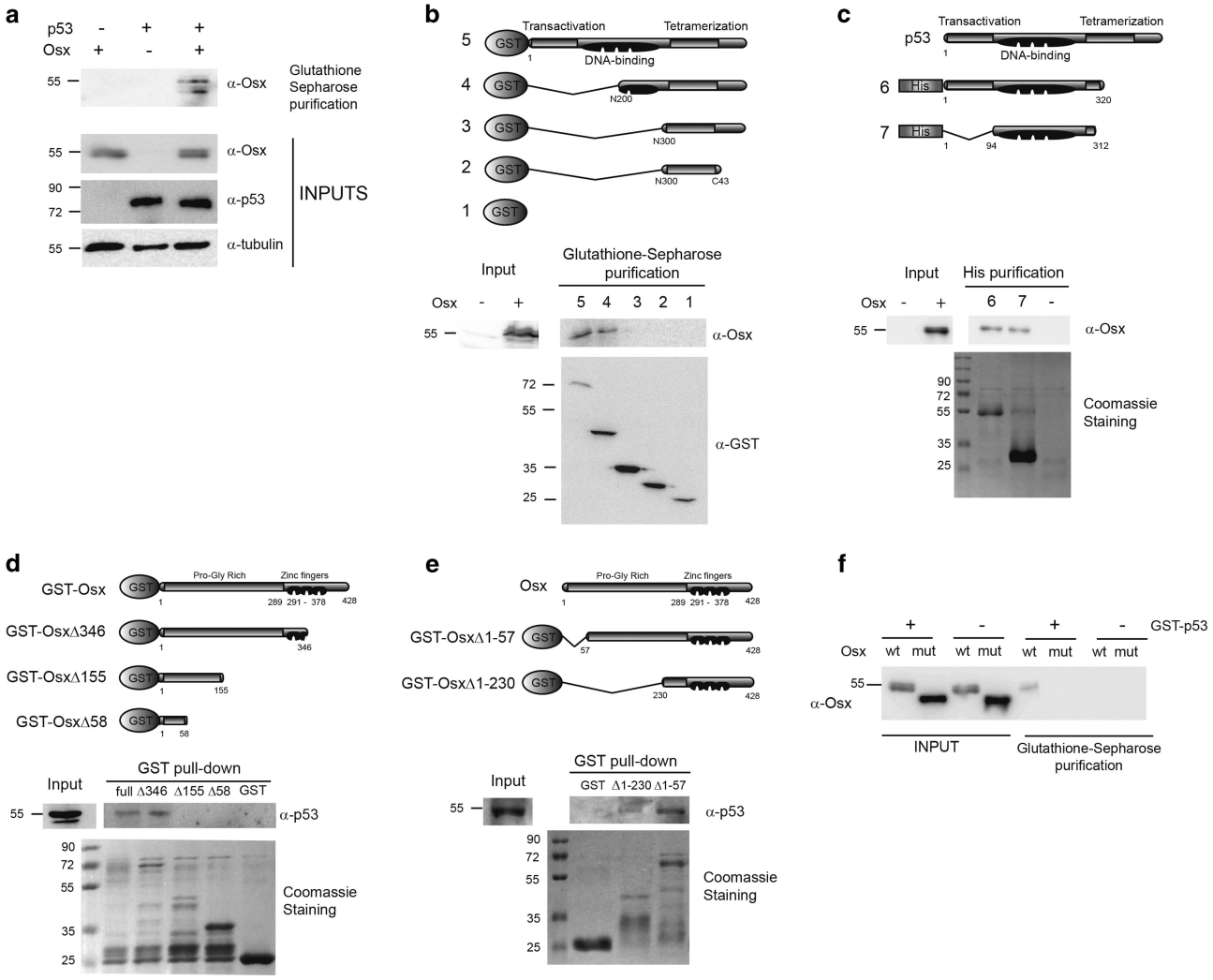

Figure 2 p53 protein physically interacts with OSX. (**a**) SaOs2 cells were infected with retroviral expression vectors for human Osx and/or GST-tagged human p53. Extracts from cells and Glutathione-Sepharose co-precipitated proteins were visualised by immunoblotting using anti-p53 and anti-Osx antibodies. (**b**) Extracts from HEK293T cells transfected with *Osx* expression vector in combination with the indicated GST-p53-chimeric protein were incubated with Glutathione-Sepharose beads for 1 h. Co-precipitated proteins were identified by immunoblotting using anti-OSX antibody. (**c**–**e**) Cell extracts were incubated with the indicated chimeric protein bound to Glutathione-Sepharose (**d** and **e**) or Ni^{2+} (**c**) beads overnight. Interacting proteins were identified by immunoblotting using anti-p53 or anti-OSX antibodies. (**f**) Lysates from HEK293T cells expressing murine wild-type *Osx* or the double mutant S73A/S77A in combination with the p53-chimeric protein or GST were incubated with Glutathione-Sepharose beads. Interacting proteins were identified by immunoblotting using anti-OSX antibody

assess this, we retrovirally infected SaOs2 cells with OSX and GST-tagged p53 expression vectors. OSX co-purified with p53, suggesting that they interact in osteogenic cells (Figure 2a). To map the involved interaction sites, we expressed *Osx* in combination with different truncated GST-p53 expression vectors in mammalian cells. OSX was able to bind to the N-terminal region of p53 protein in intact cells (Figure 2b). We further pinpoint the p53 domain involved in such interaction by studying OSX binding to recombinant N-terminal truncated p53 (Figure 2c). Altogether, the data demonstrate that the p53 DNA-binding domain is sufficient for physical interaction with OSX. We also verified which domain of OSX was involved in the interaction. Our results showed that p53 requires a region that encompasses part of the transactivation domain proximal to the OSX zinc fingers (Figures 2d and e). We also determined whether the activation status of OSX influences its interaction with p53. A less active form of OSX (the OSX S73A/S77A mutant, which cannot be phosphorylated by MAP kinases) showed lower interaction with p53 in intact cells (Figure 2f).

Similar assays with GST-p53 expression vectors showed that RUNX2 was able to bind to the N-terminal domain of p53 in mammalian cells (Supplementary Figure 2A). Recombinant truncated RUNX2 proteins showed that RUNX2 requires the PST region to physically interact with p53 (Supplementary Figure 2B).

Osx transcriptional activity is inhibited by interaction with p53. We next assessed the effect of p53 interaction on OSX transcriptional activity. We evaluated the expression

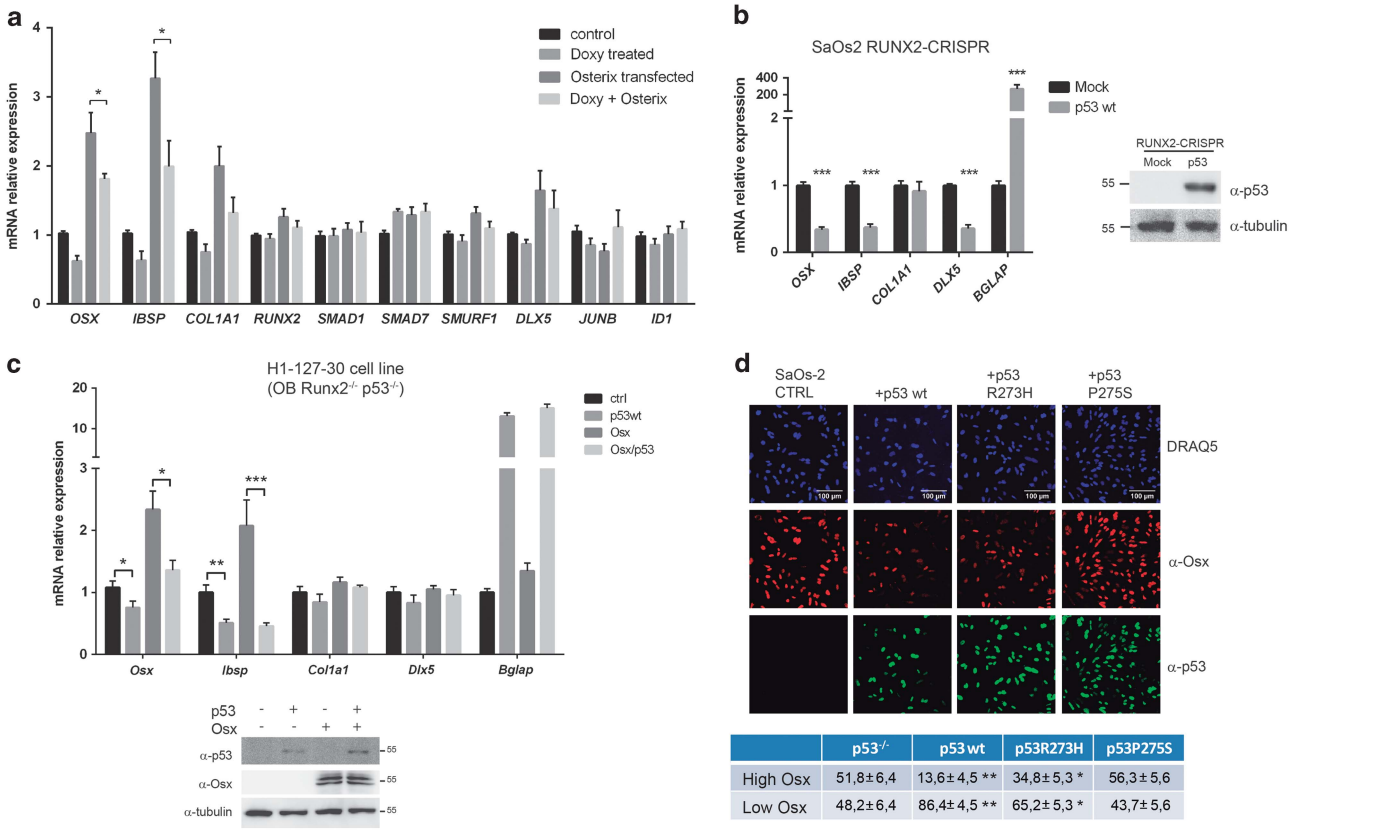

	p53-/-	p53 wt	p53R273H	p53P275S
High Osx	51,8± 6,4	13,6± 4,5 **	34,8± 5,3 *	56,3± 5,6
Low Osx	48,2± 6,4	86,4± 4,5 **	65,2± 5,3 *	43,7± 5,6

Figure 3 p53 regulates osteoblastic gene expression inhibiting OSX transcriptional activity. (**a**) mRNA expression levels in SaOs2-p53TetOn treated for 24 h with 2 nM doxycycline and/or transfected with *Osx* expression vector. mRNA was measured by qRT-PCR, normalized to *TBP* and expressed as relative expression ± S.E.M. of at least three independent experiments. (**b**) mRNA expression levels in SaOs2 *RUNX2*-CRISPR cells retrovirally infected with murine p53 expression vector. Right panel shows a western blotting to verify p53 expression. (**c**) H1-127-30 osteoblasts generated from the double *Runx2* and *Trp53* knockout mice were infected with retroviral expression vectors for murine p53 and OSX. mRNAs were measured by RT-qPCR, normalized to *TBP* and expressed as relative expression ± S.E.M. from six independent experiments. (**d**) Immunocytofluorescence of SaOs2 cells infected with retroviral expression vectors carrying murine p53 wild type, human p53R273H and murine p53P275S. Immunostaining was performed with anti-OSX and anti-p53 antibodies and nuclei visualized using DRAQ5. Quantification of OSX relative expression levels (cut-off point at <150 OSX intensity) are expressed as percentage of cells. Statistics were performed against the p53 knockout condition. (*$P<0.05$, **$P<0.01$, ***$P<0.001$ using the Student's *t*-test)

of genes implicated in the osteoblastic differentiation programme on SaOs2-p53TetOn cells overexpressing OSX in combination with doxycycline treatment (Figure 3a). Both controls and cells overexpressing OSX had a lower induction of OSX target genes (such as *OSX* itself and *IBSP*[27,31]) when p53 was expressed. The qPCR assay only detected endogenous *OSX* expression; thus, these data provide additional evidence of OSX regulation of its own promoter.[31] These observations suggest that OSX transcriptional activity is inhibited by p53.

p53 has been shown to repress RUNX2 function.[23] For this reason, we then analyzed whether the effects of p53 on osteogenic gene expression were derived from inhibition of RUNX2 or also depended on the inhibition of OSX transcriptional activity. Two distinct approaches were performed: first, generation of pools of SaOs2 cells, which are p53-deficient, where the third exon of the *RUNX2* gene was inactivated by CRISPR technology (Supplementary Figure 3A). Second, analysis of the osteoblast cell line H1-127-30 generated from the double *Runx2*/*p53* knockout mice.[32] The *RUNX2*-specific CRISPR deletion was confirmed by immunoblot, obtaining a pool of cells with 60% reduction of RUNX2 levels (Supplementary Figure 3B). Expression of p53 in these cells still conferred a strong downregulation of osteogenic genes (Figure 3b). Similarly, re-expression of p53 in *Runx2*$^{-/-}$ *p53*$^{-/-}$ osteoblasts led to inhibition of *Osx* and *Ibsp* expression, and abolished their induction by ectopic OSX (Figure 3c). Altogether, these data suggest that the inhibitory effects of p53 on osteogenic gene expression depend not only on RUNX2 but also on OSX inhibition.

We also analyzed by immunofluorescence whether p53 could block OSX trafficking to the nucleus. First, we visualized that OSX expression in SaOs2-p53TetOn cells was localized in the nucleus regardless of p53 expression. Second, at the single-cell level the expression of p53 was negatively correlated with that of OSX (Supplementary Figure 4). To further confirm the negative correlation between p53 and OSX protein levels, we infected p53-deficient SaOs2 cells with retrovirus expressing murine wild-type p53, the human contact mutant p53R273H or the murine structural mutant p53P275S. Whereas the p53R273H changes the Arg273 involved in base recognition, p53P275S (corresponding to P278S in the human p53 gene) alters the structure of the its DNA-binding domain.[33–35] Expression of wild-type p53 or the p53R273H

mutant induced a strong downregulation of endogenous OSX expression, whereas the p53P275S mutant did not significantly changed OSX levels (Figure 3d).

Osx–DNA binding is blocked by p53 protein. A mechanism by which p53 could inhibit OSX transcriptional activity could be affecting its affinity for DNA. We evaluated the OSX ability to bind to Sp1/GC-rich sequences (which have been shown to be OSX responsive elements[12,26] by performing an oligo-pull-down assay using a sequence of the bone enhancer from the *Col1a1* promoter.[26] We expressed OSX in *Trp53* knockout osteoblasts using retrovirus and tested the affinity of OSX for the oligonucleotide. Co-infection with a murine wild-type p53 retrovirus led to a 60–70% lower OSX binding affinity for the Sp1/GC-rich sites (Figure 4a). We also co-infected the p53-deficient osteoblasts with the transcriptionally inactive human p53R273H mutant. Co-expression of this mutant also reduced OSX binding to the oligonucleotide, which refutes the possibility of a p53-dependent transcriptional mechanism underlying OSX binding inhibition (Figure 4a). These results *in vitro* were confirmed by chromatin immunoprecipitation (ChIP) in SaOs2, where expression of wild-type p53 reduced OSX and RUNX2 occupancy in the responsive regions of the promoter of their target genes *IBSP*, *COL1A1* and *BGLAP* (Figure 4b). Expression of the human p53R273H mutant also reduced recruitment of OSX to *IBSP*, *COL1A1* and *BGLAP* promoters, whereas OSX binding was not significantly reduced by p53P275S (Figure 4b).

In accordance with it, the expression levels of the OSX target genes were repressed by the presence of murine wild-type p53 and the human p53R273H contact mutant in *Trp53* knockout osteoblast (Figure 4c). However, p53P275S failed to induce repression of these genes. To verify the mechanism that confers differential inhibition of OSX activity by distinct p53 mutants, we analyzed the physical interaction of OSX with wild-type p53, and the R273H and P275S mutants. Purification of OSX from extracts of SaOs2 cells retrovirally expressing *Osx* and *p53* mutants demonstrate that physical interaction between OSX and p53P275S was reduced compared with the interaction with wild type and R273H mutant (Figure 4d). These results confirm that the effects on OSX transcriptional activity are not dependent on p53 transcriptional activity, but on protein-protein interaction. Together, these data suggest regulation of OSX transcriptional activity by p53 at protein level via blockage of the OSX interaction with their Sp1/GC-rich responsive sites.

The OSX interaction network is inhibited by p53. It has recently been described that OSX acts as a cofactor for the DLX transcription factor family.[10] As p53 binds close to the OSX zinc-finger domain implicated in the OSX–DLX5 interaction, we investigated the impact of p53 binding on the OSX–DLX5 complex. First, we analyzed whether p53 could disrupt the OSX–DLX5 complex. We performed GST-DLX5 pull-down assays using extracts from SaOs2-p53TetOn cells infected with murine wild-type p53 or the human R273H mutant. As previously described OSX bound DLX5,[10] but both wild type p53 and the R273H mutant disrupted this interaction (Figure 5a). Thus, p53 could likely inhibit OSX transcriptional activity in promoters regulated by the OSX–DLX complex.

As mentioned before, OSX is able to regulate its own promoter[31] and our group had also previously identified DLX5 as an activator of the proximal promoter of *Osx*.[11] The *Osx* promoter $-114/-51$ contains a Sp1/GC-rich box that could be a target for direct OSX binding, as well as a DLX5-binding homeobox. Luciferase assays using this *Osx* promoter region showed that both OSX and DLX5 activated the *Osx* promoter, and they showed an additive effect when expressed together (Figure 5b). More importantly, activation of the *Osx* promoter was repressed by p53. Mutation of either the homeobox or the Sp1/GC-rich sequences reduced the ability of DLX5 and OSX to activate transcription from the *Osx* promoter, suggesting that both sites are relevant for their function. To further discern whether the inhibition of p53 on the *Osx* promoter is through inhibition of OSX binding to the GC-rich box or instead by avoiding its role as a DLX5 cofactor, we performed an oligo-pull-down assay using the $-114/-51$ *Osx* promoter. We tested the capacity of OSX and DLX5 to bind to the wild-type $-114/-51$ sequence (pOsx HB-wt), or to the sequence with the homeobox site mutated (pOsx HB-mut) (Figure 5c). Assays from doxycycline-treated SaOs2-p53TetOn cells confirmed that OSX was able to bind to this promoter region probably using the Sp1/GC-rich box, besides binding to the homeobox, given that OSX was still able to bind to the HB-mut oligonucleotide. As expected, DLX5 bound to the HB-wt and showed lower affinity to the HB-mut oligonucleotide. The presence of p53 not only reduced OSX binding to both sequences but also blocked the binding of DLX5 to the homeobox site. These results were confirmed by chromatin-immunoprecipitation in SaOs2-p53TetOn cells, where induction of p53 strongly reduced DLX5 occupancy in the *Osx* promoter (Figure 5d). Therefore, binding of both DLX5 and OSX to their sites were inhibited by p53. Altogether, our results suggest a novel mechanism of OSX regulation, as summarized in Figure 6. p53 inhibits OSX transcriptional and osteogenic activity by binding close to its zinc-finger region, repressing its interaction with DNA and its transcriptional partners, such as DLX5.

Discussion

Cell differentiation and proliferation are usually thought of as antagonistic events in many cell types, with differentiation being only possible after blockage of proliferation. As a canonical tumour suppressor, p53 is supposed to inhibit proliferation but also promote differentiation.[36] However, the inhibitory role of p53 in osteogenic differentiation, in a cell-autonomous manner, is well established by mouse genetics and cell-based approaches.[19] Although the p53-null mouse shows enhanced bone mineral density, Mdm2-conditional knockout results in a severe impairment of bone formation.[17,24] Interestingly, MSCs derived from induced pluripotent stem cells from Li–Fraumeni patients carrying the transcriptionally inactive p53G245D mutation showed deficient osteoblast differentiation. Moreover, deletion of p53 in these iPS cells eliminated the osteogenic differentiation defect suggesting that osteogenic effects are derived from gain-of-function activities of mutant p53.[37]

Despite this evidence, the exact nature of the mechanisms that underlie these p53 effects remained unknown. Our work identifies these effects on osteoblast differentiation through repression of OSX activity by direct interaction with p53. Previous studies focused on the impact of the p53 family over osteogenic BMP signalling with interesting findings such as

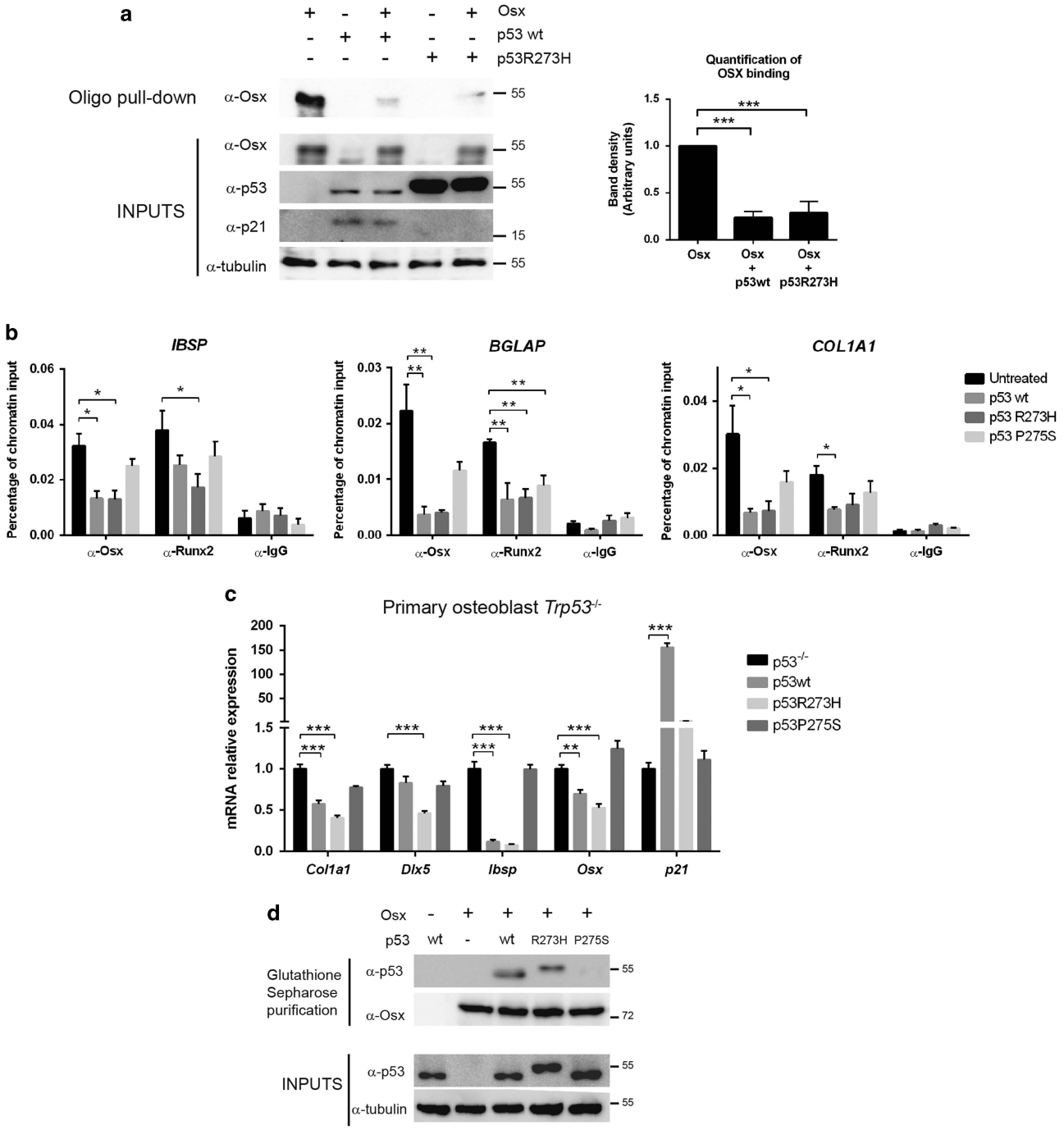

Figure 4 p53 blocks OSX binding to Sp1 elements. (**a**) Oligo-pull-down assay was performed using a biotinylated-oligonucleotide containing the *Col1a1* bone-enhancer sequence. The oligonucleotide was incubated with extracts from *Trp53* knockout primary osteoblasts retrovirally infected with the indicated expression vectors. Bar graph on the right shows the quantification of the OSX band after streptavidin-purification relative to their input levels. (**b**) ChIP from SaOs2 cells infected with retroviral expression vectors for murine p53 wild-type, human p53R273H and murine p53P275S. DNA–protein complexes were isolated with antibodies against Osx, Runx2 and IgG. Specific primers for the promoters of *IBSP*, *BGLAP* (Osteocalcin) and *COL1A1* bone-enhancer were used for qRT-PCR analysis. Results are represented relative to input chromatin. (**c**) *Trp53* knockout primary osteoblasts were retrovirally infected with murine p53 wild-type or p53P275S or human p53R273H mutant forms. *p21* gene was used as reporter of p53 transcriptional activity. mRNA was measured by qRT-PCR, normalized to *Tbp* and expressed as relative expression ± S.E.M. of at least three independent experiments (*$P<0.05$, **$P<0.01$, ***$P<0.001$, using Student's *t*-test). (**d**) SaOs2 cells were infected with retrovirus expression vectors for murine GST-tagged Osx and p53 wild-type and P275S from mouse or human p53R273H. Extracts from SaOs2 cells and Glutathione-Sepharose co-precipitated proteins were visualised by immunoblotting using anti-p53 and anti-Osx antibodies

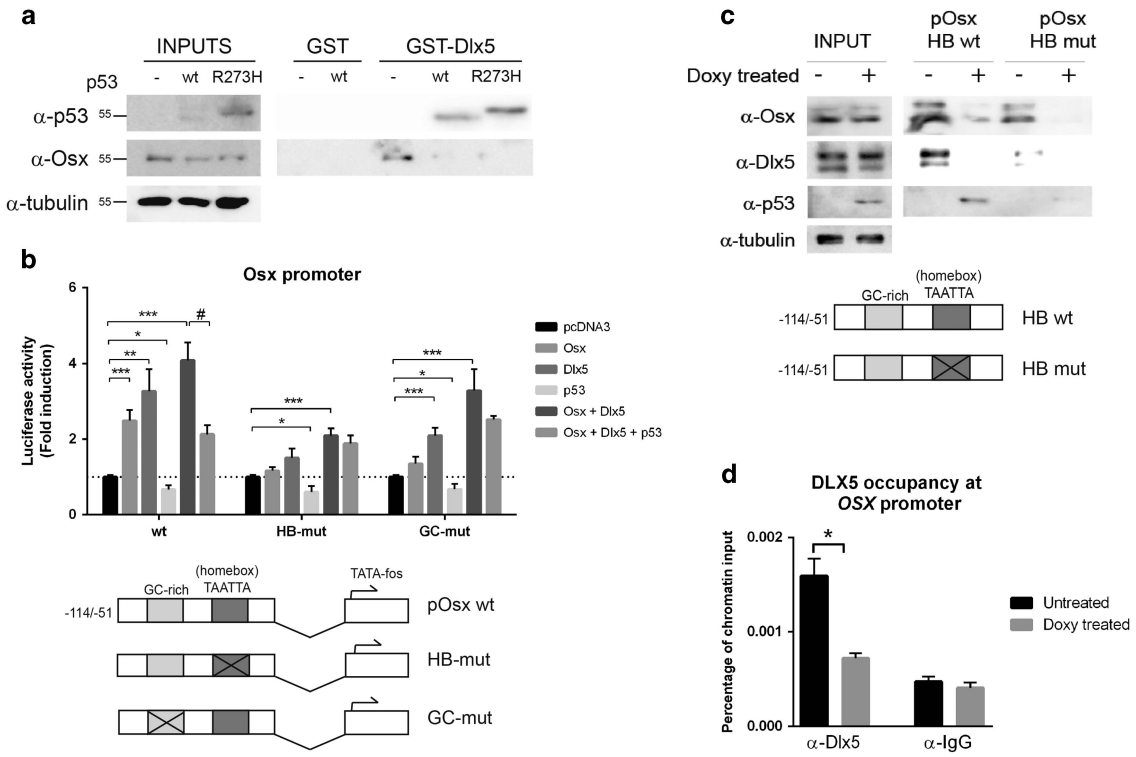

Figure 5 Inhibition of *Osx* promoter is mediated by p53 blocking DLX5-OSXx complex. (**a**) Extracts of SaOs2-p53TetOn retrovirally infected with the indicated p53-expression vectors were incubated with the indicated chimeric protein bound to Glutathione-Sepharose beads overnight. Interacting proteins were identified by immunoblotting using anti-Osx and anti-p53 antibodies. (**b**) SaOs2 cells were co-transfected with the indicated expression vectors, or empty pcDNA3 vector as control, and the murine −114/−51 Osterix-promoter luciferase reporter, wild-type or with the indicated mutated versions. HB-mut is the reporter with the homeodomain box mutated; GC-mut indicates mutation in the Sp1/GC-rich box.[11] Scheme of the −114/−51 Osterix-promoter is shown. Luciferase activity was measured and normalized against *β*-galactosidase activity, and represented as fold induction compared with the pcDNA3 transfection condition. # is used to compare Osx+Dlx5 *versus* Osx+Dlx5+p53 conditions. (**c**) Oligo-pull down using biotinylated −114/−51 Osterix-promoter sequence (pOsx HB wt) and its homeobox-mutated version (pOsx HB mut). Extracts from SaOs2-p53TetOn untreated or treated for 24 h with 2 nM doxycycline were used. Interacting proteins were identified by immunoblotting using anti-OSX, anti-DLX5 and anti-p53. (**d**) SaOs2-p53TetOn were treated or not with 2 nM doxycycline for 24 h. DNA-protein complexes were isolated with antibodies against DLX5 and IgG. Specific primers for the *Osx* promoter were used for qRT-PCR analysis. Results are represented relative to input chromatin from three independent experiments (*$P<0.05$)

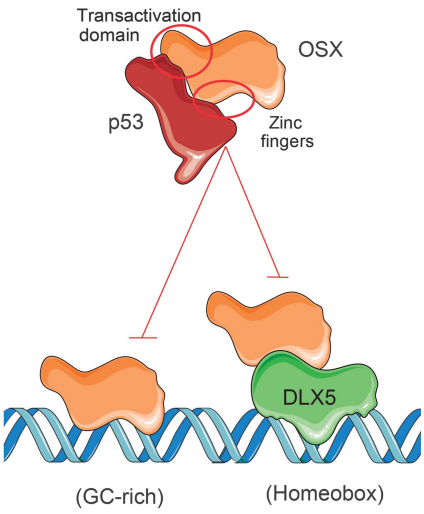

Figure 6 Schematic representation of the proposed p53-OSX network: p53 blocks Osterix transcriptional activity by physical interaction. We suggest that p53-OSX interaction prevents OSX from binding to Sp1/GC-rich sequences, and also interferes in the formation of the OSX–DLX5 transcriptional complex, that responds to homeobox sequences

the p53-Smad1/5 physical interaction,[38] or Smad1 upregulation due to the lack of p53.[16,20] Our data suggest that these changes were of low magnitude. We also identified positive regulation of the gene expression of the Smad signalling inhibitor *Smad7*. These data are in agreement with data from epithelial cells, which establishes that p53 family members bind to the *Smad7* promoter through a p53-response element.[39]

As mentioned above, our work and previous studies revealed that p53 represses the expression of osteoblast-determining transcription factors independently of p53–DNA binding.[17,37] Our data further demonstrated the ability of p53 to inhibit the transcriptional osteogenic programme independent of p53–DNA binding on the basis of several lines of evidence. First, a transcriptionally inactive mutant form of human p53 (R273H) similarly blocked OSX function, whereas a murine conformational mutant (P275S) had lower inhibitory ability. Second, RUNX2-deficient osteoblasts were also sensitive to the inhibitory effects of p53. Third, p53 was able to repress binding to DNA and cooperative transcriptional effects of endogenous and ectopic OSX and DLX5.

Osx, *Runx2* and *Dlx5* are mandatory transcriptional regulators of the osteogenic process. Their gene products

physically interact and lead to a strong cooperation in the transcription of target genes and the production of a mineralized bone matrix.[9,10] Previous studies also depict an integrative feed-forward transcriptional network involving *Runx2*, *Osx* and *Dlx5*, in which they positively regulate each other´s transcription.[9,11,40–43] These fully integrated relationships suggest that any alteration in the function of any of them would result in a de-regulation of the whole network. Thus, the p53-mediated inhibition of OSX function could be an important factor in the maintenance of bone homeostasis under physiological conditions. p53 signalling mutations, which lead to high p53 protein expression levels,[44,45] would disturb the function of the *Dlx5-Runx-Osx* network with important consequences.

The DNA-binding domain of p53 interacts with an OSX domain adjacent to its zinc fingers. Similarly, we also mapped the PST transactivation domain of RUNX2 as its p53-interaction region. Interaction between p53 and OSX results in downregulation of *Osx* target genes involved in bone matrix maturation, such as *Ibsp*, *Col1a1* and *Osx* itself. The *Osx* proximal promoter, the first known molecular target of p53 inhibition,[17] is positively controlled through direct DNA binding by OSX and DLX5 proteins.[11,27,31] We determined that p53 interaction does not alter OSX localization but impairs OSX–DNA binding *in vitro* and *in vivo* to their canonical Sp1/GC-rich sites. Moreover, p53 also inhibits OSX–DLX5 transcriptional complex formation and binding to homeobox sequences. Importantly, the OSX–DLX5 complex co-occupy most the bone enhancer regions in genome-wide analysis and evolutionary analysis showed correlation with the evolution of skeletal formation.[10] As p53 and DLX5 share the region of interaction with OSX,[10] it is plausible to infer that higher levels of p53 would abrogate OSX–DLX5 complex formation. By blocking these two DNA-binding mechanisms of action of OSX, p53 breaks two important mechanisms of the osteoblast transcriptional programme.

Our findings that p53 has a transcriptionally independent role in OSX function suggest important physiopathological consequences. Proliferation and differentiation should co-exist in a coordinated manner to maintain tissue homeostasis over time. Besides its major role in the transcriptional control of proliferation and apoptosis, p53 might block osteogenic differentiation from mesenchymal precursors to allow its expansion and prevent their shortage from premature specification. Deregulation of these networks would lead to osteoporosis by shortage of mesenchymal precursors and/or misdirected differentiation towards alternative fates such as adipocytes, which are both characteristic features of ageing.[46] Several reports indicate that loss of osteogenic potential and increased adipogenesis of bone progenitors during senescence is dependent on p53 and correlated with lower *Osx* expression.[47] Moreover, the shift from osteoblastogenesis to increased adiposity observed in osteopenias induced by ageing, accelerated senescence or ovariectomy correlated with upregulation of p53 levels.[46]

The relation between p53 mutations and osteosarcomagenesis has been highlighted in several studies.[36,48,49] Osteosarcoma is largely composed of poorly differentiated cells[50] and the p53 loss-of-function is enough for the development of osteosarcoma.[51] Previous studies, aimed at detecting the origin of the osteosarcoma, point to dedifferentiated osteoblastic cells, rather than MSCs.[36,37,49,50] In addition, most p53 mutations are missense and impair DNA binding, but give rise to the gain of new oncogenic functions.[52,53] Our data suggest a possible negative correlation between p53 and OSX protein levels that varies depending on p53 specific mutation (Figure 3d). Therefore, the definition of p53 status and its mutation in osteosarcomas likely could help us to understand its effect on osteogenic differentiation, and to better tackle the progression of the disease. Altogether, our data support a model where p53 represses OSX–DNA binding and OSX–DLX5 interaction and thereby deregulates the osteogenic transcriptional network.

Materials and Methods

Mouse model. *Trp53* knockout mice B6.129S2-*Trp53*tm1Tyj/J from Jackson Laboratories (Bar Harbor, ME, USA) were kindly provided by Dr J Martin-Caballero. Mice were housed under controlled conditions (12 h light/12 h dark cycle, 21 °C, 55% humidity) and fed *ad libitum* with water and a 14% protein diet (Teklad 2014, Harlan, Santa Perpètua de Mogoda, Barcelona, Spain). All animal experiments were performed in accordance with guidelines approved by the Ethical Committee for Animal Experimentation of the University of Barcelona and Generalitat de Catalunya (Spain).

Cell culture. SaOs2-p53TetOn, kindly provided by Dr R Bartrons, and HEK293T (American Type Culture Collection, Rockville, MD, USA) cell lines were maintained in DMEM supplemented with 10% fetal bovine serum (FBS), 2 mM glutamine, 1 mM pyruvate, 100 U/ml penicillin and 0.1 mg/ml streptomycin. The isolation of primary osteoblasts from calvaria was carried out as described previously.[54] Primary osteoblasts and H1-127-30 osteoblast cell line [32] were maintained in α-MEM supplemented with 10% FBS, 2 mM glutamine, 1 mM pyruvate, 100 U/ml penicillin and 0.1 mg/ml streptomycin. As osteogenic differentiation medium, osteoblast medium was supplemented with 50 μM ascorbic acid and 10 mM β-glycerophosphate. HEK293T cells were transiently transfected using polyethylenimine, and SaOs2 using Lipofectamine-LTX (Invitrogene). Retroviral infection in *Trp53* knockout osteoblasts, H1-127-30 and SaOs2 cells were performed as described previously.[55] Doxycycline treatment (2 nM) was carried out in media with 1% FBS. BMP2 (R&D, Minneapolis, MN, USA) was used at 2 nM.

CRISPR-Cas9. The *RUNX2* gene was knocked down in SaOs2 cells using the system described by Ran *et al.*[56]. The gRNA sequence was designed to target the exon 3 of the *RUNX2* gene. The guide sequence was cloned into the pSpCas9(BB)-2A-Puro vector donated by R. Estevez and confirmed by sequencing. The primers used were: F:5′CACCGGCTGGTGCTCGGATCTACGG3′ and R:5′-AAACCCG TAGATCCGAGCACCAGCC-3′. SaOs2 cells were plated in six wells and transfected overnight. An empty vector without gRNA was used as negative control. Puromycin was added at 1 μg/ml and maintained three days for selection. The selected cells were tested for *RUNX2* gene deletion by endonuclease assay. The following primers were used for *RUNX2* amplification: F:5′-CAAACTTGATTTCTCACCTCCTCA-3′ and R:5′-TTCAAGGTAAGAGGCTACACCGC-3′. The positive pools were expanded and checked for RUNX2 knock-down by immunoblot.

Plasmids and reagents. Murine Osterix expression vectors were kindly provided by Dr B de Crombrugghe. The Osx S73A/S77A, GST-Osx, GST-OsxΔ346 and GST-OsxΔ155 GST-Dlx5 were previously described,[9,12] and GST-OsxΔ58, GST-OsxΔ1–57 and GST-OsxΔ1–230 were generated by double digestion from GST-Osx. GST-Runx2 and GST-Runx2Δ230 were kindly provided by Dr M Montecino. The GST-p53 and their derivatives were kindly provided by Dr Y Xiong. The human His-p53-(1–320) and His-p53-(94–312) were a gift from Dr Arrowsmith (Addgene plasmid 24864 and 24866, respectively). The pMXs-p53 and pMXs-p53P275S from mouse were a gift from Dr Yamanaka (Addgene plasmids 22725 and 22726, respectively).[57] The pMXs-p53R273H was generated from pLenti6/V5-p53_R273H (from Dr Futscher, Addgene plasmid 22934)[58] by subcloning the human p53R272H sequence into pMXs plasmid. Human pMXs-Osx was a gift from Dr O Mazda. The pBABE-GST-p53 retroviral expression vector

was generated from pEBG-GST-p53. The pBABE-GST-OSX was generated from pGEX-Osx.

Pull-down assays. For *in vitro* GST-pull down experiments, the assays were performed as described previously.[9] For analysis of the physical interaction assays in mammalian cells, the GST-p53 or the GST-Osx vectors were co-transfected with *Osx* or the distinct p53 mutant expression vectors in HEK293T or retrovirally infected in SaOs2 cells and cells were lysed after 48 h. Lysates were collected, centrifuged to eliminate debris and purified by binding to Glutathione-Sepharose beads for 1 h at 4 °C. Then, the beads were washed with washing buffer (50 mM Tris/HCl, 150 mM NaCl, 0.1% Igepal-CA630 plus protease and phosphatase inhibitors) three times. Bound proteins were detected by immunoblotting. For *in vitro* pull down of His-tagged proteins, all used buffers were supplemented with 10 mM imidazol and bound to Ni^{2+} resin for purification.

Luciferase assay. SaOs2 cells were cultured in 24-well plates and transfected for 8 h with Lipofectamine LTX with the indicated plasmids. Transfection efficiency was assessed by GFP expression. Luciferase activities were quantified 48 h post-transfection using the Luciferase assay system (Promega, Madison, WI, USA) and normalized using the β-Galactosidase Detection Kit II (Clontech, Mountain View, CA, USA).

Oligo-pull-down assays. Oligo-pull-down assays were carried out as previously described.[26] The pOsx HB-wt and pOsx HB-mut oligonucleotides were generated by PCR using biotinylated primers from the proximal Osterix murine promoter, and wild-type or homeobox-mutated $-114/-51$ *Osterix* promoter sequences as templates. The Sp1 oligonucleotide sequence was generated from the *Col1a1* promoter as previously described.[26]

Western blot assay. Identification of proteins, from cell extracts or pull-down assays, was performed by immunoblotting against phospho-Smad1/5/8, Smad1 (Cell Signaling 9743 and 13820, Danvers, MA, USA), Osx (Abcam 22552, Cambridge, UK), Runx2 (MBL D130-3, Woburn, MA, USA), p53 (Cell Signaling 48818), Id1 (C-20 sc-488) and p21 (C-19 sc-397) (Santa Cruz Biotechnology, Dallas, TX, USA) or α-tubulin (Sigma-Aldrich T5168, St. Louis, MO, USA), diluted at 1 : 1000. Antibodies against Dlx5 (C-20 sc-18152 and Y-20 sc-18151) (Santa Cruz Biotechnology) were used at 1 : 500. Immunoreactive bands were detected with horseradish-peroxidase-conjugated secondary antibodies and an ECL-kit (Biological Industries, Cromwell, CT, USA).

ChIP assay. ChIP assay was carried out as described in Artigas *et al.*[9]. $SaOs_2$ p53TetOn cells were cultured until confluence before overnight doxycycline treatment. $SaOs_2$ were retrovirally infected with the distinct p53 mutant constructs. ChIP was carried out using 1 μg of the indicated antibodies: anti-Osx (Abcam), anti-Runx2 (MBL), anti-Dlx5 (C-20 sc-18152 and Y-20 sc-18151, 0.5 μg each) or anti-IgG (Upstate) as a control, and purified with 20 μl Magna ChIP Protein A+G Magnetic Beads (Millipore, Billerica, MA, USA). The DNA fragments were purified using the QIAquick Gel Extraction Kit (Qiagen, Hilden, Germany) and analyzed by qRT-PCR. The primers used for the qRT-PCR analysis for *IBSP* and *COL1A1* were previously described.[9] *BGLAP* primers were R: 5′-CCGTAGGCCAAACCCCAG AGGATATGT-3′ and F: 5′-CTCTGCTTGAACCTATTTTAGGTCTCTGA-3′. *OSX* primers were: R: 5′-CCTGCTTCCCACCCCTTCCA-3′ and F: 5′-ATGAGGAGG GCGAGAGAGGG-3′.

Immunocytofluorescence. SaOs2 p53TetOn immunofluorescence was performed as previously described[9] using 1 : 100 p53 (Cell Signaling) and 1:250 anti-Osterix (Abcam).

qRT-PCR analysis. Total RNA was isolated from primary osteoblasts or SaOs2 cells using TRIsure reagent (Bioline, London, UK). Purified RNA was reverse-transcribed using the High-Capacity cDNA Reverse Transcription Kit (Applied Biosystems, Foster City, CA, USA). Quantitative PCRs were carried out using the ABI Prism 7900 HT Fast Real-Time PCR System and Taqman 5′-nuclease probes (Applied Biosystems). Designed Taqman assays (Applied Biosystems) were used to quantify gene expression. All transcripts were normalized to *Tbp* expression.

Statistical analysis. Statistical analysis was performed using the Student's *t*-test. Quantitative data are presented as means $\pm$ S.E.M. Differences were considered significant at $^{*}P<0.05$, $^{**}P<0.01$ and $^{***}P<0.001$.

Conflict of Interest

The authors declare no conflict of interest.

Acknowledgements. We thank Drs B de Crombrugghe, J Martín-Caballero, M Montencino, Y-Xiong and HM Ryoo for reagents. We also thank E Adanero, E Castaño and B Torrejón for technical assistance. Natalia Artigas is the recipient of a fellowship from University of Barcelona. This research was supported by grants from the M.E.C. (BFU2014-56313-P) and La Marató de TV3.

1. Long F. Building strong bones: molecular regulation of the osteoblast lineage. *Nat Rev Mol Cell Biol* 2011; **13**: 27–38.
2. Karsenty G, Kronenberg HM, Settembre C. Genetic control of bone formation. *Annu Rev Cell Dev Biol* 2009; **25**: 629–648.
3. Sinha KM, Zhou X. Genetic and molecular control of osterix in skeletal formation. *J Cell Biochem* 2013; **114**: 975–984.
4. Ducy P, Zhang R, Geoffroy V, Ridall AL, Karsenty G. Osf2/Cbfa1: a transcriptional activator of osteoblast differentiation. *Cell* 1997; **89**: 747–754.
5. Zhou X, Zhang Z, Feng JQ, Dusevich VM, Sinha K, Zhang H *et al.* Multiple functions of Osterix are required for bone growth and homeostasis in postnatal mice. *Proc Natl Acad Sci USA* 2010; **107**: 12919–12924.
6. Baek WY, de Crombrugghe B, Kim JE. Postnatally induced inactivation of Osterix in osteoblasts results in the reduction of bone formation and maintenance. *Bone* 2010; **46**: 920–928.
7. Timpson NJ, Tobias JH, Richards JB, Soranzo N, Duncan EL, Sims AM *et al.* Common variants in the region around Osterix are associated with bone mineral density and growth in childhood. *Hum Mol Genet* 2009; **18**: 1510–1517.
8. Lapunzina P, Aglan M, Temtamy S, Caparros-Martin JA, Valencia M, Leton R *et al.* Identification of a frameshift mutation in Osterix in a patient with recessive osteogenesis imperfecta. *Am J Hum Genet* 2010; **87**: 110–114.
9. Artigas N, Urena C, Rodriguez-Carballo E, Rosa JL, Ventura F. Mitogen-activated protein kinase (MAPK)-regulated interactions between Osterix and Runx2 are critical for the transcriptional osteogenic program. *J Biol Chem* 2014; **289**: 27105–27117.
10. Hojo H, Ohba S, He X, Lai LP, McMahon AP. Sp7/osterix is restricted to bone-forming vertebrates where it acts as a Dlx co-factor in osteoblast specification. *Dev Cell* 2016; **37**: 238–253.
11. Ulsamer A, Ortuno MJ, Ruiz S, Susperregui AR, Osses N, Rosa JL *et al.* BMP-2 induces Osterix expression through up-regulation of Dlx5 and its phosphorylation by p38. *J Biol Chem* 2008; **283**: 3816–3826.
12. Ortuno MJ, Ruiz-Gaspa S, Rodriguez-Carballo E, Susperregui AR, Bartrons R, Rosa JL *et al.* p38 regulates expression of osteoblast-specific genes by phosphorylation of osterix. *J Biol Chem* 2010; **285**: 31985–31994.
13. Greenblatt MB, Shim JH, Zou W, Sitara D, Schweitzer M, Hu D *et al.* The p38 MAPK pathway is essential for skeletogenesis and bone homeostasis in mice. *J Clin Invest* 2010; **120**: 2457–2473.
14. Carvajal LA, Manfredi JJ. Another fork in the road–life or death decisions by the tumour suppressor p53. *EMBO Rep* 2013; **14**: 414–421.
15. Molchadsky A, Shats I, Goldfinger N, Pevsner-Fischer M, Olson M, Rinon A *et al.* p53 plays a role in mesenchymal differentiation programs, in a cell fate dependent manner. *PLoS ONE* 2008; **3**: e3707.
16. Liu H, Jia D, Li A, Chau J, He D, Ruan X *et al.* p53 regulates neural stem cell proliferation and differentiation via BMP-Smad1 signaling and Id1. *Stem Cells Dev* 2013; **22**: 913–927.
17. Wang X, Kua HY, Hu Y, Guo K, Zeng Q, Wu Q *et al.* p53 functions as a negative regulator of osteoblastogenesis, osteoblast-dependent osteoclastogenesis, and bone remodeling. *J Cell Biol* 2006; **172**: 115–125.
18. Armstrong JF, Kaufman MH, Harrison DJ, Clarke AR. High-frequency developmental abnormalities in p53-deficient mice. *Curr Biol* 1995; **5**: 931–936.
19. He Y, de Castro LF, Shin MH, Dubois W, Yang HH, Jiang S *et al.* p53 loss increases the osteogenic differentiation of bone marrow stromal cells. *Stem Cells* 2015; **33**: 1304–1319.
20. Ruan X, Zuo Q, Jia H, Chau J, Lin J, Ao J *et al.* P53 deficiency-induced Smad1 upregulation suppresses tumorigenesis and causes chemoresistance in colorectal cancers. *J Mol Cell Biol* 2015; **7**: 105–118.
21. Liu W, Qi M, Konermann A, Zhang L, Jin F, Jin Y. The p53/miR-17/Smurf1 pathway mediates skeletal deformities in an age-related model via inhibiting the function of mesenchymal stem cells. *Aging (Albany NY)* 2015; **7**: 205–218.
22. Ozaki T, Wu D, Sugimoto H, Nagase H, Nakagawara A. Runt-related transcription factor 2 (RUNX2) inhibits p53-dependent apoptosis through the collaboration with HDAC6 in response to DNA damage. *Cell Death Dis* 2013; **4**: e610.

23. van der Deen M, Taipaleenmaki H, Zhang Y, Teplyuk NM, Gupta A, Cinghu S *et al.* MicroRNA-34c inversely couples the biological functions of the runt-related transcription factor RUNX2 and the tumor suppressor p53 in osteosarcoma. *J Biol Chem* 2013; **288**: 21307–21319.
24. Lengner CJ, Steinman HA, Gagnon J, Smith TW, Henderson JE, Kream BE *et al.* Osteoblast differentiation and skeletal development are regulated by Mdm2-p53 signaling. *J Cell Biol* 2006; **172**: 909–921.
25. Nakashima K, Zhou X, Kunkel G, Zhang Z, Deng JM, Behringer RR *et al.* The novel zinc finger-containing transcription factor osterix is required for osteoblast differentiation and bone formation. *Cell* 2002; **108**: 17–29.
26. Ortuno MJ, Susperregui AR, Artigas N, Rosa JL, Ventura F. Osterix induces Col1a1 gene expression through binding to Sp1 sites in the bone enhancer and proximal promoter regions. *Bone* 2013; **52**: 548–556.
27. Yang Y, Huang Y, Zhang L, Zhang C. Transcriptional regulation of bone sialoprotein gene expression by Osx. *Biochem Biophys Res Commun* 2016; **476**: 574–579.
28. Chen H, Hays E, Liboon J, Neely C, Kolman K, Chandar N. Osteocalcin gene expression is regulated by wild-type p53. *Calcif Tissue Int* 2011; **89**: 411–418.
29. Chen H, Kolman K, Lanciloti N, Nerney M, Hays E, Robson C *et al.* p53 and MDM2 are involved in the regulation of osteocalcin gene expression. *Exp Cell Res* 2012; **318**: 867–876.
30. Chau JF, Jia D, Wang Z, Liu Z, Hu Y, Zhang X *et al.* A crucial role for bone morphogenetic protein-Smad1 signalling in the DNA damage response. *Nat Commun* 2012; **3**: 836.
31. Barbuto R, Mitchell J. Regulation of the osterix (Osx, Sp7) promoter by osterix and its inhibition by parathyroid hormone. *J Mol Endocrinol* 2013; **51**: 99–108.
32. Lee KS, Kim HJ, Li QL, Chi XZ, Ueta C, Komori T *et al.* Runx2 is a common target of transforming growth factor beta1 and bone morphogenetic protein 2, and cooperation between Runx2 and Smad5 induces osteoblast-specific gene expression in the pluripotent mesenchymal precursor cell line C2C12. *Mol Cell Biol* 2000; **20**: 8783–8792.
33. de Vries A, Flores ER, Miranda B, Hsieh HM, van Oostrom CT, Sage J *et al.* Targeted point mutations of p53 lead to dominant-negative inhibition of wild-type p53 function. *Proc Natl Acad Sci USA* 2002; **99**: 2948–2953.
34. Chen Y, Dey R, Chen L. Crystal structure of the p53 core domain bound to a full consensus site as a self-assembled tetramer. *Structure* 2010; **18**: 246–256.
35. Cho Y, Gorina S, Jeffrey PD, Pavletich NP. Crystal structure of a p53 tumor suppressor-DNA complex: understanding tumorigenic mutations. *Science* 1994; **265**: 346–355.
36. Kruiswijk F, Labuschagne CF, Vousden KH. p53 in survival, death and metabolic health: a lifeguard with a licence to kill. *Nat Rev Mol Cell Biol* 2015; **16**: 393–405.
37. Lee DF, Su J, Kim HS, Chang B, Papatsenko D, Zhao R *et al.* Modeling familial cancer with induced pluripotent stem cells. *Cell* 2015; **161**: 240–254.
38. Balboni AL, Cherukuri P, Ung M, DeCastro AJ, Cheng C, DiRenzo J. p53 and DeltaNp63alpha coregulate the transcriptional and cellular response to TGFbeta and BMP signals. *Mol Cancer Res* 2015; **13**: 732–742.
39. De Rosa L, Antonini D, Ferone G, Russo MT, Yu PB, Han R *et al.* p63 Suppresses non-epidermal lineage markers in a bone morphogenetic protein-dependent manner via repression of Smad7. *J Biol Chem* 2009; **284**: 30574–30582.
40. Roca H, Phimphilai M, Gopalakrishnan R, Xiao G, Franceschi RT. Cooperative interactions between RUNX2 and homeodomain protein-binding sites are critical for the osteoblast-specific expression of the bone sialoprotein gene. *J Biol Chem* 2005; **280**: 30845–30855.
41. Lee MH, Kim YJ, Yoon WJ, Kim JI, Kim BG, Hwang YS *et al.* Dlx5 specifically regulates Runx2 type II expression by binding to homeodomain-response elements in the Runx2 distal promoter. *J Biol Chem* 2005; **280**: 35579–35587.
42. Nishio Y, Dong Y, Paris M, O'Keefe RJ, Schwarz EM, Drissi H. Runx2-mediated regulation of the zinc finger Osterix/Sp7 gene. *Gene* 2006; **372**: 62–70.
43. Kawane T, Komori H, Liu W, Moriishi T, Miyazaki T, Mori M *et al.* Dlx5 and mef2 regulate a novel runx2 enhancer for osteoblast-specific expression. *J Bone Miner Res* 2014; **29**: 1960–1969.
44. Muller PA, Vousden KH. p53 mutations in cancer. *Nat Cell Biol* 2013; **15**: 2–8.
45. Vijayakumaran R, Tan KH, Miranda PJ, Haupt S, Haupt Y. Regulation of mutant p53 protein expression. *Front Oncol* 2015; **5**: 284.
46. Sui B, Hu C, Liao L, Chen Y, Zhang X, Fu X *et al.* Mesenchymal progenitors in osteopenias of diverse pathologies: differential characteristics in the common shift from osteoblastogenesis to adipogenesis. *Sci Rep* 2016; **6**: 30186.
47. Despars G, Carbonneau CL, Bardeau P, Coutu DL, Beausejour CM. Loss of the osteogenic differentiation potential during senescence is limited to bone progenitor cells and is dependent on p53. *PLoS ONE* 2013; **8**: e73206.
48. Velletri T, Xie N, Wang Y, Huang Y, Yang Q, Chen X *et al.* P53 functional abnormality in mesenchymal stem cells promotes osteosarcoma development. *Cell Death Dis* 2016; **7**: e2015.
49. Quist T, Jin H, Zhu JF, Smith-Fry K, Capecchi MR, Jones KB. The impact of osteoblastic differentiation on osteosarcomagenesis in the mouse. *Oncogene* 2015; **34**: 4278–4284.
50. Tang N, Song WX, Luo J, Haydon RC, He TC. Osteosarcoma development and stem cell differentiation. *Clin Orthop Relat Res* 2008; **466**: 2114–2130.
51. Walkley CR, Qudsi R, Sankaran VG, Perry JA, Gostissa M, Roth SI *et al.* Conditional mouse osteosarcoma, dependent on p53 loss and potentiated by loss of Rb, mimics the human disease. *Genes Dev* 2008; **22**: 1662–1676.
52. Muller PA, Vousden KH. Mutant p53 in cancer: new functions and therapeutic opportunities. *Cancer Cell* 2014; **25**: 304–317.
53. Kim MP, Zhang Y, Lozano G. Mutant p53: multiple mechanisms define biologic activity in cancer. *Front Oncol* 2015; **5**: 249.
54. Rodriguez-Carballo E, Ulsamer A, Susperregui AR, Manzanares-Cespedes C, Sanchez-Garcia E, Bartrons R *et al.* Conserved regulatory motifs in osteogenic gene promoters integrate cooperative effects of canonical Wnt and BMP pathways. *J Bone Miner Res* 2011; **26**: 718–729.
55. Gamez B, Rodriguez-Carballo E, Graupera M, Rosa JL, Ventura F. Class I PI-3-kinase signaling is critical for bone formation through regulation of SMAD1 activity in osteoblasts. *J Bone Miner Res* 2016; **31**: 1617–1630.
56. Ran FA, Hsu PD, Wright J, Agarwala V, Scott DA, Zhang F. Genome engineering using the CRISPR-Cas9 system. *Nat Protoc* 2013; **8**: 2281–2308.
57. Kitamura T, Koshino Y, Shibata F, Oki T, Nakajima H, Nosaka T *et al.* Retrovirus-mediated gene transfer and expression cloning: powerful tools in functional genomics. *Exp Hematol* 2003; **31**: 1007–1014.
58. Junk DJ, Vrba L, Watts GS, Oshiro MM, Martinez JD, Futscher BW. Different mutant/wild-type p53 combinations cause a spectrum of increased invasive potential in nonmalignant immortalized human mammary epithelial cells. *Neoplasia* 2008; **10**: 450–461.

Supplementary Information accompanies this paper on Cell Death and Differentiation website (http://www.nature.com/cdd)